Arch. Pharm. Res. (2020) 43:134–152
https://doi.org/10.1007/s12272-020-01208-3

Online ISSN 1976-3786
Print ISSN 0253-6269

Archives of Pharmacal Research
www.springer.com/12272

REVIEW

Emerging NIR light-responsive delivery systems based on lanthanide-doped upconverting nanoparticles

Xuan Thien Le[1] · Yu Seok Youn[1]

Received: 18 November 2019 / Accepted: 9 January 2020 / Published online: 24 January 2020

Abstract Together with the development of nanoscience, lanthanide (Ln)-doped upconversion nanoparticles (UCNPs), which can emit UV/VIS light upon irradiation by near-infrared laser sources, is emerging as one of the most favorable materials in the field of nanomedicines. Light-responsive drug delivery is known as an efficient strategy to achieve temporal and spatial controlled drug release. Compared to conventional light-sensitive drug delivery systems, UCNPs are endowed with many advantages, such as deeper tissue penetration and low toxicity. With their unique properties, UCNPs not only serve as potential optical probes for bioimaging but also perform a critical role in therapeutic applications through photon-triggered mechanisms. In particular, UCNPs in combination with different materials and delivery strategies could overcome therapy resistance and enhance therapeutic effectiveness. This article focuses on the current achievements in the last decade of modification methods, diagnostics, and designs of UCNP-based nanoplatforms for successful phototherapy, chemotherapy, and bioimaging.

Keywords Upconversion nanoparticle · Lanthanide · Delivery system · Phototherapy · Bioimaging

✉ Yu Seok Youn
ysyoun@skku.edu

[1] School of Pharmacy, Sungkyunkwan University, 2066 Seobu-ro, Jangan-gu, Suwon, Gyeonggi-do 16419, Republic of Korea

Introduction

The increasing number of people with cancer, together with the millions of deaths it causes every year, renders it one of the most serious health problems and burdens in human society. For the purpose of addressing this issue, a huge number of efforts have been spent to the development and the clinical application of novel cancer therapies. However, limited success has been attained due to the poor targeting ability, systemic toxicity, and drug resistance of conventional cancer therapies. Smart drug delivery strategies are essential in overcoming these challenges. An ideal drug delivery system (DDS) should release the active pharmaceutical ingredients with precise dosing and spatiotemporal control. Therefore, stimuli-responsive DDSs have attracted a great deal of attention (Mura et al. 2013). Compared to internal stimuli-responsive strategies, the external ones, comprising temperature, magnetic field, electrical field, light, and ultrasound responsive DDSs, have the advantages of reducing inter-patient variability and provide a feasible approach to precise drug delivery. Of these external stimuli, near-infrared (NIR) light is emerging as a salient trigger for biomedical applications because it rarely impairs the physiological function of normal cells (Guo and You 2017). However, numerous conventional photosensitizers (PSs), such as organic dyes, semiconductor nanomaterials or metal complexes, still have several limitations depriving them of being approved for clinical use. For example, quantum dots and fullerenes exhibit high toxicity (Tsoi et al. 2013; Youn et al. 2017); semiconductor crystals such as TiO_2 require excitation by UV/VIS light with poor tissue penetration properties (Wang et al. 2018a); organic dyes are challenged by the requirements of high energy and the high intensity of excitation sources and by the photobleaching phenomenon (Zheng et al. 2012).

Upconversion (UC) emission is a nonlinear optical process in which the subsequent absorption of no less than two photons resulting in the emission at a shorter wavelength than the excitation wavelength (Auzel 2004). The concept was first introduced in the year 1959 by Nicolaas Bloembergen (Bloembergen 1959). Despite considerable potential, the application of UC focused on crystalline materials or bulk glass for the next few decades (Pacheco and De Araujo 1988; Tanabe et al. 1992) without any significant influence in the field of biomedicine. It was not until the 1990s, together with the rapid development of nanoscience and luminescence mechanisms, that the design, synthesis, and bio-application of upconversion nanoparticles (UCNPs) was well established. UCNPs have considerable advantages, such as resistance to photobleaching, low toxicity, and deep tissue penetration, which can deal with the limitations of the aforementioned photosensitizers. Since the structure design and nanochemistry of UCNPs are well studied, they can be further engineered for specific bio-applications, not only as probes for diagnostics but also in therapeutic applications. In fact, thanks to the unique properties of UCNPs, they have emerged as one of the most promising materials for versatile nanocarriers in drug delivery.

This review presents a comprehensive account of the recent progress in lanthanide (Ln)-doped UCNPs. At first, an overview of the UC mechanisms and nanochemistry of Ln-doped UCNPs are described. Then, we demonstrate the designs and bio-applications of these novel nanoplatforms in both bioimaging and cancer therapy, implying their extraordinary versatility and great potential. Finally, the outlook of the future development of UCNPs is discussed.

Overview of Ln-doped UCNPs

Upconversion processes can simply be divided into four mechanisms, these include excited-state absorption (ESA), energy transfer UC (ETU), photon avalanche (PA), and energy-migration-mediated upconversion (EMU) (Auzel 2004), as shown in Fig. 1. Different from the two-photon emission phenomenon, which involves the simultaneous absorption of two photons (Drobizhev et al. 2011; Lin and Vučković 2010; Rumi and Perry 2010), UC emission requires metastable energy levels to act as the platforms for consecutively absorbed photons.

Rare-earth elements often exist in the most stable state as trivalent ions (Cheisson and Schelter 2019), with partially filled 4f orbitals shielded by completely filled $5s^2$ and $5p^6$ that exhibit numerous electronic energy states ranging from IR to UV. This makes lanthanide ions an ideal host lattice for UCNPs. Each Ln-doped UCNP has an exclusive energy transfer process involving the combination of two or more mechanisms described above.

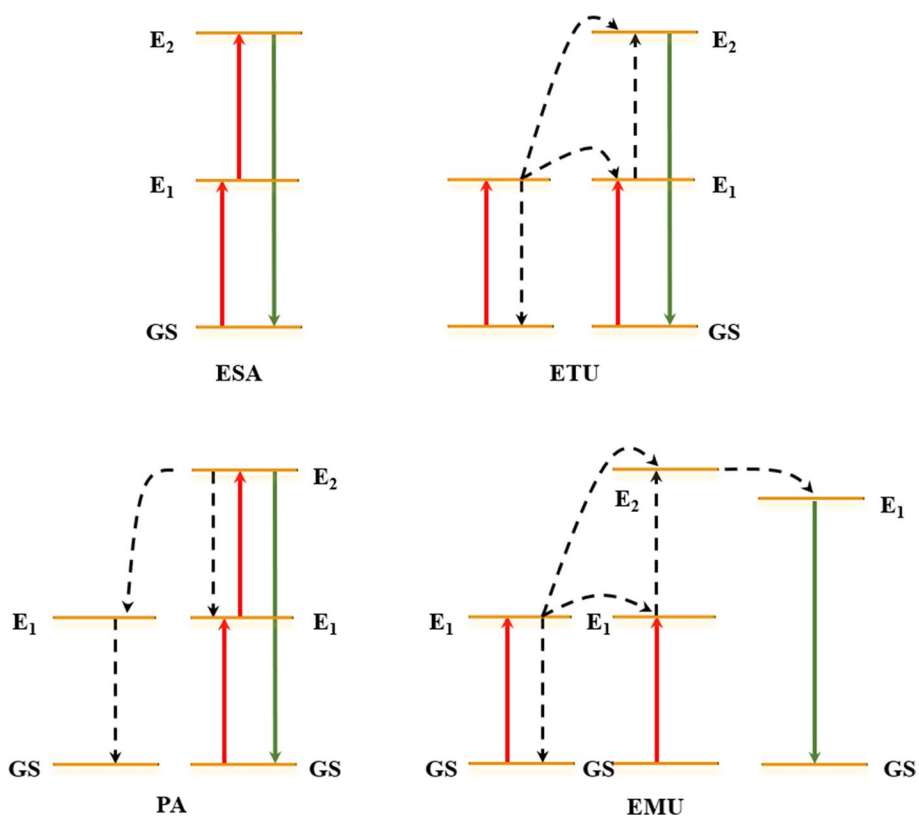

Fig. 1 Primary upconversion mechanism of Ln-doped UCNPs (E_1, E_2: excited states; GS: ground state). Reorganized from Duan et al. (2018)

Ln-doped UCNPs consist of two main components: dopants and a suitable host matrix to embed the dopants. Dopants usually act as the luminescence center and can be categorized into sensitizers and activators. Under appropriate excitation, sensitizers obtain higher energetic states followed by the non-radiative transfer of energy to other nearby dopant ions. After a complicated energy transfer or single excitation process, the activators gradually accumulate enough energy for the anti-Stoke type emission.

Regularly, Yb^{3+} is chosen as the sensitizer owing to its single energy transition between the ground state and $^2F_{5/2}$ excited state with the absorption band in the NIR spectrum (980 nm). In addition, the $^2F_{7/2} \rightarrow {}^2F_{5/2}$ transition matches well with several f-f transitions of typical activators such as Tm^{3+}, Er^{3+}, and Ho^{3+}. The sensitizer content has a remarkable influence on the optical properties of UCNPs. It should be high enough to allow the energy transfer between sensitizers and activators, but not so high that it leads to detrimental cross relaxation, which causes UC quenching. The doping ratio of the sensitizer is often kept at 20 to 40 mol%. In addition, Nd^{3+} can also be co-doped with Yb^{3+} as a sensitizer to achieve an absorption peak at about 800 nm (Fig. 2) (Shen et al. 2013). This benefits the bio-application of Ln-doped UCNPs because water strongly absorbs the NIR 980 nm light, generates heat, and hinders the effect of the laser source in deep tissues. The use of 800 nm sensitized UCNPs is a good approach to overcome these limitations.

For an activator candidate, a long lifespan of metastable excited states is necessary. The longer time that an electron stays at a specific intermediate energy level, the higher chance that it can be excited again by the non-radiative emission from another dopant. On the other hand, activators should also have ladder-like energy levels with similar energy gaps. Tm^{3+}, Er^{3+}, and Ho^{3+} ions with suitable energy levels are now becoming the most common choices for activators. To prevent the concentration of fluorescent quenching, a low doping concentration of activators, 0.5–3 mol%, is required.

The host matrices have a decisive impact on the upconversion luminescence (UCL) efficiency of UCNP by controlling spatial distance and energy transfer efficiency between dopants. There are a few considerations for the selection of a crystal matrix. The first is size similarity between matrix cations and dopant ions. In general, all tripositive rare-earth ions have similar ionic sizes and chemical properties, making them ideal host matrix cations. Another high demand for host materials is a low lattice phonon energy to minimize non-radiative interactions and strengthen radiative emissions. In comparison to oxides and heavy halides, fluorides have the advantage of exhibiting low phonon energies and high chemical stability. Hence, $NaYF_4$ is widely used as a host material for Ln-doped nanocrystals. UCNPs with a $NaYF_4$ host matrix can exist as either α-phase or β-phase, in which β-phase UCNPs have a much higher UCL efficiency.

The primary purpose in the preparation of UC nanocrystals is to successfully control UCL, nanoparticle size, and colloidal stability. Nowadays, the synthesis of UC nanocrystals has been meticulously studied in various synthetic methods such as thermal decomposition (Boyer et al. 2006; Mai et al. 2006, 2007; Li and Zhang 2008), solvothermal (Wang et al. 2005b, 2009; Wang and Li 2007; Cao et al. 2011), coprecipitation (Yi et al. 2004), ionothermal (Liu et al. 2009), and sol–gel (Patra et al. 2003). Of these, thermal decomposition is the most popular way to synthesize UC nanocrystals and produces good quality UCNPs. However, the difficulty in attaining reproducible synthesis, toxic byproducts, costly materials, as well as restricted reaction conditions, impede the use of thermal decomposition in commercial systems. Compared to thermal decomposition, the co-precipitation method does not require extremely high reaction temperature and generates lower toxic by-products. However, these benefits are outweighed by the relatively

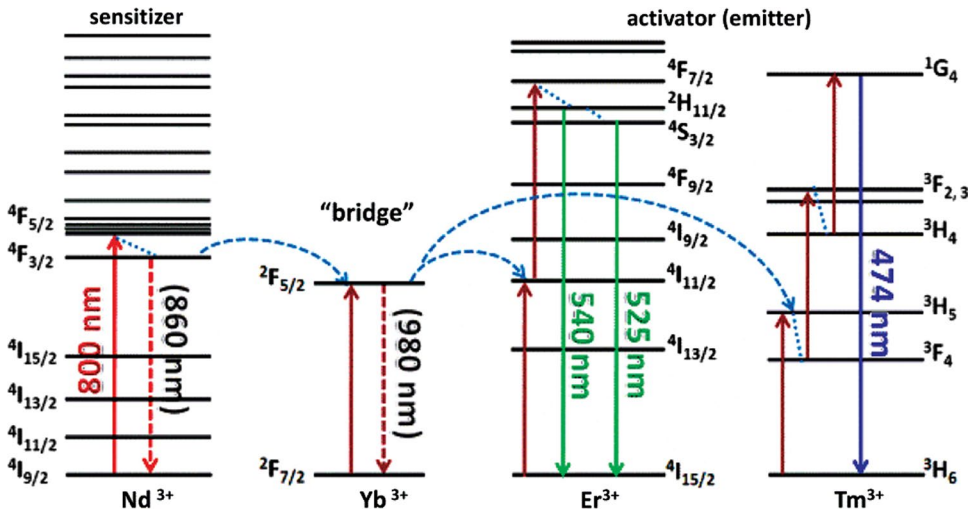

Fig. 2 UC processes Yb/Tm/Nd- and Yb/Er/Nd- doped nanocrystals under 800 nm laser irradiation. (Reprinted with permission from (Shen et al. 2013). Copyright © 2013 WILEY-VCH Verlag GmbH & Co. KGaA, Weinheim)

low quality of prepared UCNPs, which requires an annealing process to obtain UCNPs with desired optical properties. More recently, a solvothermal method is emerging as a promising approach to transcend any conventional techniques. Solvothermal is considered as a friendly synthetic method with lower reaction temperature and lower toxic byproducts. Furthermore, by using this method, the size and shape of UCNPs can be practically controlled, and thus it produces good UCNPs with low cost. All of the aforementioned techniques have been well described by researchers around the world and reviewed in the literature (Li and Lin 2010; Gai et al. 2013; Johnson and van Veggel 2013; Chen et al. 2014a; Li et al. 2015; Lingeshwar Reddy et al. 2018).

Due to the focus of this review, details about UC nanocrystal synthesis are not covered. Instead, we will discuss the fabrication of Ln-doped nanocrystal-based composite for application in the field of biomedicine. In fact, most UCNPs are endowed with a hydrophobic capping ligand at the outermost side acting as a stabilizer during UCNP synthesis. To be suitable for use in biological systems, several surface modifications and the integration of functional moieties are needed to obtain hydrophilic UCNPs that can be well dispersed in physiological conditions and further engineered to conjugate biomolecules. Briefly, there are six strategies for preparing hydrophilic UCNPs via surface modification, namely ligand exchange, ligand removal, ligand oxidation, ligand interaction, layer-by-layer deposition, and silica coating (Table 1). In the ligand exchange method, hydrophobic caps are replaced by more hydrophilic agents to form UCNPs that is well dispersed in aqueous solvents. Despite the simple operation, this process often requires a large excess amount of the hydrophilic ligands, high temperatures and long reaction time to prevent the incomplete ligand exchange, which results in non-well-defined surface chemistry. Ligand-free UCNPs can be obtained after treating oleic acid (OA) caps with strong acids or $NOBF_4$. This method provides UCNPs with long-term stability in hydrophilic solvents, for example, acetonitrile and dimethylformamide, as well as makes the way for a subsequent ligand exchange step either with hydrophobic or hydrophilic ligands. On the other hand, by using Lemieux-von Rudloff reagent, the doubled bond at the C9 position of OA can be oxidized and expose carboxylic acid residue to the surface without any significant effect on size or morphology of UCNPs. However, the yielded water-dispersible UCNPs perform a decrease in the UCL intensity due to the precipitation of MnO_2 after a long reaction time (Naccache et al. 2009). The ligand interaction approach involves the hydrophobic-hydrophobic interaction between the fatty acid chain on the surface of UCNPs and the hydrophobic alkyl chain of amphiphilic reagents or hydrophobic pocket of the host molecule. Compared to OA-capped UCNPs in cyclohexane, the second layer containing PAA, poloxamers, SDS, or CTAB show a decrease by 60–80% in the UCL intensity in water (Yi and Chow 2007; Liang et al. 2012; Wu et al. 2012). The layer-by-layer deposition method uses electrostatic interaction between positively charged and negatively charged polymer to control the charge and the thickness of the coating layer, which can be easily tuned by changing the number and the order of deposited polymers. It should be noted that the intensity of UCL decreases with the increase of the number of layers (Huang et al. 2015). Besides, a sharp fluctuation of pH value can impair the integrity of the polyelectrolyte layer, leading to the aggregation of hydrophilic UCNPs obtained from the layer-by-layer deposition process. Silica coating is a popular technique for surface modification of various materials, including UCNPs, by using typical methods for the synthesis of silica nanoparticles. The inert silica shell endows UCNPs@SiO_2 with good stability over a broad range of pH as well as avoid the release of metal ion from UCNPs. The thickness of silica coating layer can be practically controlled by controlling the concentration of silica precursors, and this shell displays the minimal influence of the UCL (Yi et al. 2004; Li et al. 2008).

Upconversion nanoplatforms in bioimaging

Bioimaging science has recently received great attention in the biomedical field owing to its impressive ability to visualize biological systems in real-time. With the aim of improving the quality of imaging data, plentiful luminescent materials, such as organic dyes, metal complexes, quantum dots, semiconductor nanomaterials, and fluorescent proteins, have been developed as biosensors or fluorescent probes. However, these single-photon excitation-based materials have several limitations. For example, the use of organic dyes is challenged by the photobleaching phenomenon, a very short emission life (less than 100 ns) and autofluorescence noise signals from biological tissue.

As a promising alternative, Ln-doped UCNPs display a large anti-Stokes shift with sharp multiline emissions, ranging from IR to UV. By precisely controlling dopants such as different combinations of dopant ions, doping concentration, and core–shell structure during UCNP synthesis, the emission peaks and relative intensities can be feasibly controlled, enabling multicolor UCL even under only one laser source. UC emission results from the electronic transition between nearby metal ions, hence UCNPs display excellent photostability (i.e., no photobleaching). Ln-doped UCNPs have maximum absorption wavelength in the NIR range, which is well-matched with the optical window for in vivo imaging (Fig. 3) (Shen et al. 2013). As a result, the excitation light can possess deep penetration, lower phototoxicity, and reduce undesired autofluorescence from biological tissues in comparison to UV or VIS irradiation. These benefits pave

Table 1 Common surface medication methods for producing hydrophilic UCNPs

	Principles	Schematic of method	Representative surface treating materials	References
Ligand exchange	Hydrophobic caps are replaced by more hydrophilic agents to form UCNPs that well dispersed in aqueous solvents		Citric acid, hexadienoic acid, 3-mercaptopropionic acid, PAA, PVP, Thiol PEG amine, PAMAM, cucurbit[7]uril	Bogdan et al. (2010), Liu et al. (2013, 2018), Xiao et al. (2014), Li et al. (2018), Sun et al. (2018), Zhang et al. (2018)
Ligand removal	Ligand-free UCNPs can be obtained after treating OA caps with strong acids or $NOBF_4$	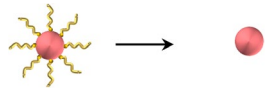	HCl (pH 4), $NOBF_4$	Peng et al. (2013), Cen et al. (2015), Zhong et al. (2015), Shi et al. (2016), Fu et al. (2017), Liang et al. (2017), Xu et al. (2017a, b)
Ligand oxidation	The doubled bond at the C9 position of OA can be oxidized and expose carboxylic acid residue to the surface	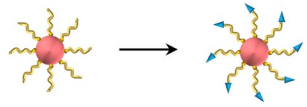	Lemieux–von Rudloff reagent MnO_4^-/IO_4^-	Chen et al. (2008), Cen et al. (2015), Wu et al. (2018)
Ligand interaction	Hydrophophic-hydrophobic interaction between the fatty acid chain on the surface of UCNPs and the hydrophobic alkyl chain of amphiphilic reagents or the hydrophobic pocket of the host molecule	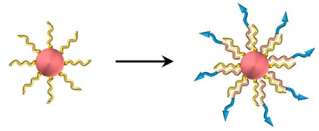	CTAB, SDS, tritonX-100, polysorbate, transferrin, α-cyclodextrin	Liu et al. (2011a), Liang et al. (2012), Seo et al. (2015), Wang et al. (2017)
Layer-by-layer deposition	Electrostatic interaction between positively charged and negatively charged polymer	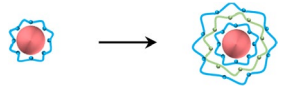	PAH/PSS/PAH, PEI/DSS, PAA/PEI	Wang et al. (2005a), Guller et al. (2015), Xiang et al. (2016), Lin et al. (2017)
Silica coating	Silica shell can be deposited on the surface of UCNPs using typical methods for the synthesis of silica nanoparticles	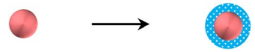	Silica	Lai et al. (2015), Lu et al. (2015), Liu et al. (2017), Lv et al. (2017), Kang et al. (2018)

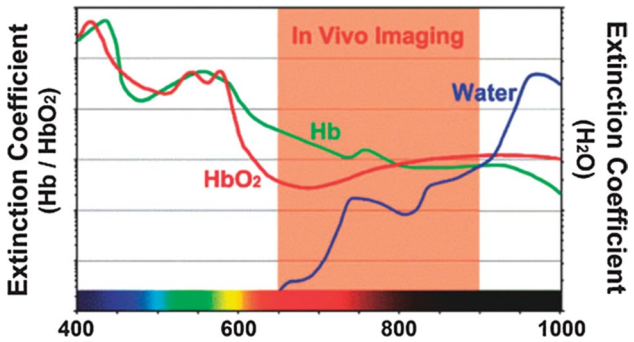

Fig. 3 Extinction coefficient of hemoglobin and water in the range from VIS to NIR light illustrating optical window for bioimaging. (Reprinted with permission from (Shen et al. 2013). Copyright © 2013 WILEY-VCH Verlag GmbH & Co. KGaA, Weinheim)

the way for the use of Ln-doped UCNPs in a huge number of bio-applications such as diagnosis, biosensing, in vivo imaging, and phototherapy.

In 2011, Liu et al. successfully prepared sub-10 nm $NaLuF_4$-based UCNPs by the thermal decomposition method. The β-$NaLuF_4$:Gd/Yb/Tm (24/20/1) nanocrystals possessed bright UCL under a continuous excitation at 980 nm and achieved high-contrast UCL in vivo imaging with a penetration depth up to 2 cm (Liu et al. 2011b). In the following year, Wang et al. used UCNPs as probes for stem cell labeling (Wang et al. 2012). Thanks to the positive surface charge, the oligo-arginine-conjugated UCNPs could be taken up more efficiently by mesenchymal stem cells compared to unconjugated UCNPs. Little nanoparticles leakage from labeled mesenchymal stem cells was observed, implying the potential for long-term cell tracking. Interestingly, ultra-high sensitivity with as few as 10 cells was reported using UCNP-embedded stem cells, whereas thousands of cells are required for quantum dots or magnetic resonance probes for in vivo imaging (Fig. 4).

In addition to luminescent imaging, magnetic resonance imaging (MRI) is also a common technique in bioimaging science. Trivalent Gd ions at the ground state have seven unpaired electrons, making it possible to use as a T_1 MRI contrast agent. Gd^{3+} can exist as host matrix cations, dopants or just be incorporated into the shell layer of UCNPs. Xing and co-workers developed ultrasmall $NaGdF_4$ nanodots for application in MRI. The $NaGdF_4$ nanocrystals were synthesized using a pyrolysis method, which produced 2.4 times more efficient MR contrasts than that of clinical Magnevit (Xing et al. 2014). Because of their ultrasmall size, ~2 nm, these nanoparticles could be filtered from the human body through urine within a short time. The chelating molecule, diethylenetriaminepentaacetic acid (DTPA), on the surface, allowed released Gd^{3+} ions to be captured to prevent systemic toxicity in vivo. Similarly, in 2015, Du et al. improved MRI sensitivity by the simultaneous incorporation of Gd^{3+}

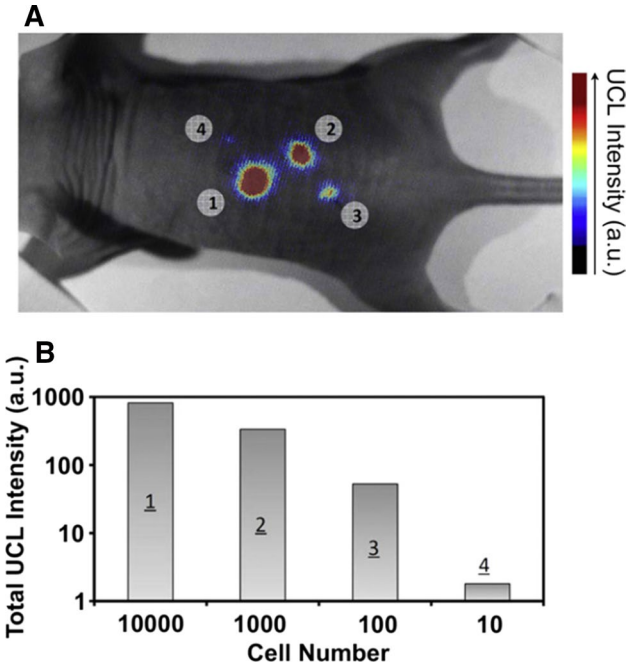

Fig. 4 Sensitivity of UCNPs probes applying in labeling mMSCs. **a** An UCL image exhibited the signals from UCNP-PEG-Arg at different numbers of mMSCs (10–10^4 cells). **b** Quantification of UCL signals. (Reprinted with permission from (Wang et al. 2012). Copyright © 2012 Elsevier)

as an internal doping ion and the external BSA·$DTPA^{Gd}$ capping of UCNPs (Du et al. 2016).

The decrease of UC efficiency by solvent relaxation in an aqueous solution is an obstacle to the application of UCNPs in biological systems for luminescence imaging. Maji and co-workers found that a UCNP/α-cyclodextrin (UCNP/α-CD) inclusion complex, which showed good dispersibility in water, could serve as a photo-acoustic imaging (PAI) probe. In comparison with OA-capped UCNPs, UCNP/α-CD under 980-nm irradiation showed UCL quenching resulting from non-radiative relaxation in aqueous solvent while the subsequent PA signal and thermal conductivity were enhanced (Maji et al. 2014). UCNP/α-CD was non-cytotoxic, blowing its chance to be utilized in PAI in vivo.

X-ray computed tomography (CT) is also a common technique in diagnostics because of its deep penetration, high resolution, and cost effectiveness. Compared to other well-established inorganic-based nanomaterials, Ln-doped UCNPs has some distinct attributes that may allow it to become an exceptional CT contrast agent. The K-edge energy of Yb is located at a higher-energy range of the X-ray spectrum that is applied recently in clinical use. As a result, patients can be exposed to a lower level of radiation, thanks to the higher intrinsic contrast. In 2012, the application of Ln-doped UCNPs in the CT technique was demonstrated by Liu and co-workers. The surface of

as-synthesized $NaYF_4$:Er UC nanocrystals was modified by DSPE-PEG2000 to yield hydrophilic UCNP-PEG for further use in vivo. It was revealed that at the equivalent concentration, the X-ray absorption of UCNP-PEG was much higher than that of iobitridol, a well-known CT contrast agent in clinical practice. In contrast to iobitridol, the long circulation time of UCNP-PEG allows it to migrate to the lymph nodes to visualize cancer metastasis by lymph node mapping. Furthermore, UCNP-PEG displayed higher CT contrast efficiency compared to Au, Bi, Pt, Ta-based nanomaterials (Liu et al. 2012b). Their study on $BaYbF_5$@SiO_2@PEG also agreed with the results described above (Liu et al. 2012c).

In the process of optimizing diagnosis accuracy, multimodal has attracted great attention. In 2011, Zhang fabricated UCNPs@SiO_2-I/PEG nanoprobes with promising in vivo dual-modal imaging. It possessed remarkable UCL properties together with enhanced CT contrast, which was attributed to the presence of rare-earth elements besides iodine (Zhang et al. 2011). Tian et al. (2015) reported another concept of the UNCP-based nanoplatform, which applied TPGS-UCNP-doxorubicin in dual-modal fluorescent/CT imaging. D-α-tocopheryl polyethylene glycol 1000 succinate (TPGS) with an amphiphilic structure acts as a stabilizer for hydrophilic UCNPs. More importantly, co-administration with TPGS endowed this UCNP with the ability to inhibit P-gp mediated multi-drug resistance (MDR). After loading doxorubicin (DOX), TPGS-UCNP-DOX could effectively treat MCF-7 tumors (Tian et al. 2015), thereby becoming a notable strategy for theranostics. A nanobiosensor for cancer diagnostics involving the switching of UCL-MR signals was developed by Lv et al. (2018). In this nanostructure, the UCL of $NaYF_4$:Yb,Er@$NaYF_4$:Yb,Nd was quenched by an outer coating of MnO_2 nanosheets. The tumor microenvironment with the enrichment of glutathione (GSH)/H_2O_2 could eliminate the MnO_2 layer by transferring it to paramagnetic Mn^{2+} ions. Hence, the UCL signal was restored and the MRI signal was generated simultaneously (Fig. 5) (Lv et al. 2018). This study proposed a potential optical probe discriminating between tumor cells and normal cells via a GSH/H_2O_2-responsive mechanism. Rieffel and co-workers introduced an epitope to achieve spatial and temporary sensitivity. They prepared UCNPs coated porphyrin-phospholipid (PoP) for hexamodal imaging. The PoP coating relates to conventional fluorescence (FL) while UCNPs can be applied to UC luminescence, PAI, and CT. Moreover, PoP or other tetrapyrrole particles can form a stable chelate with ^{64}Cu, broadening the application of PoP-UCNPs in Cerenkov luminescence (CL) and positron emission tomography (PET) (Rieffel et al. 2015). While FL and PA describe the self-assembly status of particles, CL and UC are effectively visualized at an intermediate depth, PET and CT achieve the deepest penetration (Fig. 6).

Photodynamic therapy using upconversion nanoparticles

Photodynamic therapy (PDT) is a non-invasive approach of treating cancer. It involves the administration of a photosensitizer (PS) followed by the irradiation of a laser source, which matches the excitation wavelength of the PS, at the tumor sites. After being activated, the PS transfers its energy to O_2 molecules and produces reactive oxygen species (ROS) leading to irreversible damage to tumor cells (Hwang et al. 2018; Jeon and Ko 2019; Le et al. 2018; Lucky et al. 2015). Nevertheless, not all of the PSs have an excitation wavelength in harmony with the optical window in biological tissues, weakening its efficacy in deeply localized tumor areas. As mentioned previously, UCNPs endowed with deep penetration and the ability to convert NIR light to multiline from IR to UV is a good solution to deal with the above problem.

Organic PS molecules are usually hydrophobic and can be loaded onto nanoparticles through physical adsorption (Fig. 7). The surface modification of OA-capped UCNP with zwitterionic lipids form a lipid hydrocarbon layer, which acts as a good carrier for PSs. For example, Thanasekaran reported a lipid-wrapped UC nanocomplex for NIR-mediated PDT. In this research, UCNPs were stabilized by phospholipid, EggPC and then the PSs were encapsulated through a hydrophobic interaction with the hydrocarbon fatty region (Thanasekaran et al. 2018). In 2014, Wang and co-workers developed a concept using UCNPs for the combination of PDT and gene therapy, in which chlorine-e6 (Ce6) was also loaded onto UCNPs by immersing itself into

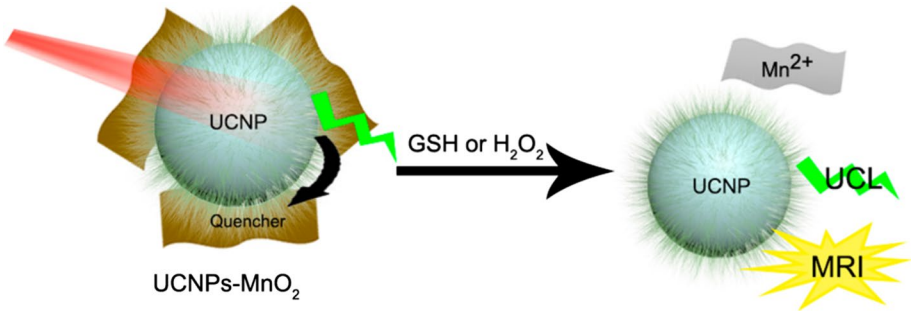

Fig. 5 Schematic illustration showing mechanism of UCNPs-based GSH/H_2O_2-repsonsive probe. (Reprinted with permission from (Lv et al. 2018). Copyright © 2018 American Chemical Society)

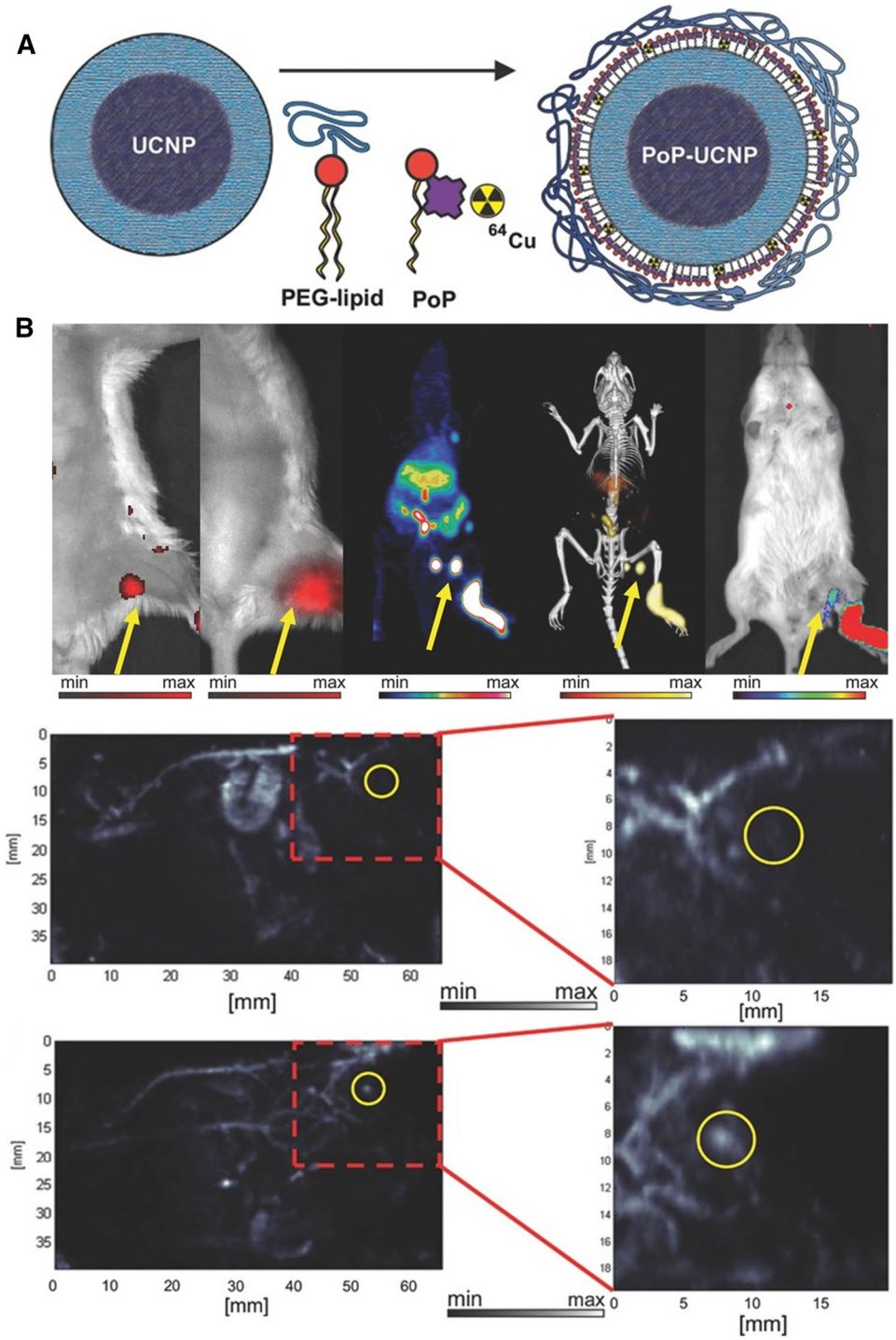

Fig. 6 Porphyrin-phospholipid (PoP)-coated UCNP for hexamodal imaging. **a** PoP-UCNP structure. **b** In vivo lymphatic imaging by using PoP-UCNPs as a versatile probe in mice. (Reprinted with permission from (Rieffel et al. 2015).Copyright © 2015 WILEY-VCH Verlag GmbH & Co. KGaA, Weinheim)

the hydrophobic oleic layer beneath the PEI/PEG coating (Wang et al. 2014). As nanoparticles are suitable for target delivery of not only drugs but also immune-regulating molecules to tumor-draining lymph nodes (Park et al. 2017), in 2019 the same delivery strategy was applied to an antigen-capturing nanoplatform used for phototherapy and immune therapy. In this study, rose bengal (RB) was loaded into a self-assembled lipid layer containing indocyanine green (ICG), DSPE-PEG-mal, and fatty acid chain on the surface of UCNPs via a hydrophobic interaction (Wang et al. 2019). Under 805-nm laser irradiation, UCNP/ICG/RB-mal exhibited efficient combination of PDT and photothermal therapy (PTT), which were attributed to RB and ICG, respectively, and killed cancer cells. Furthermore, tumor-derived protein

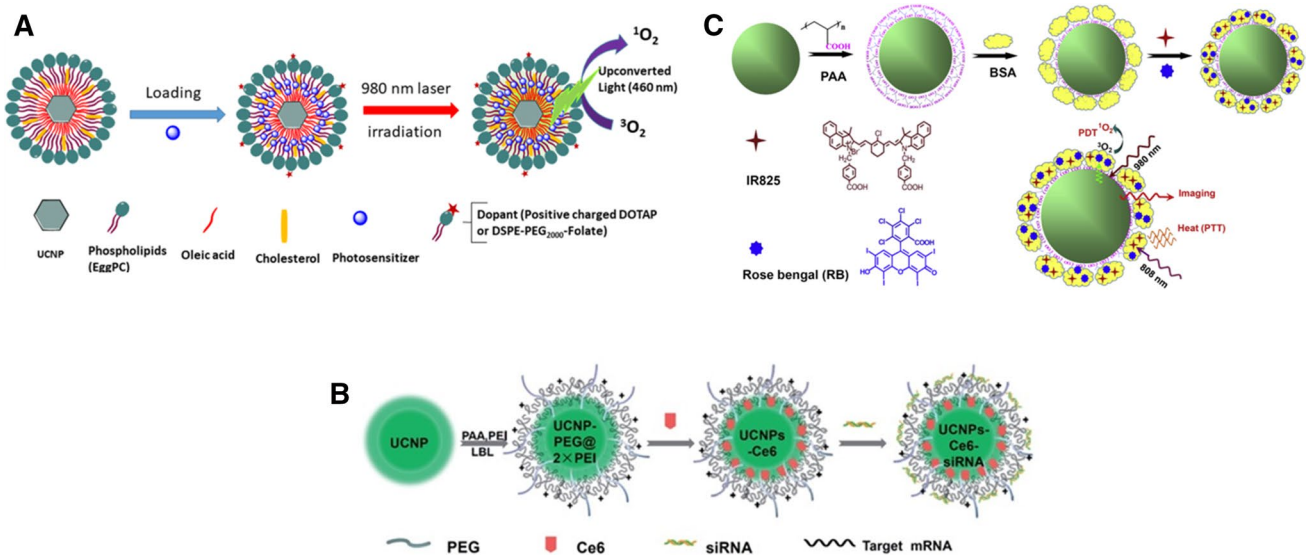

Fig. 7 Schematic of different strategies to embed PSs onto UCNPs via physical adsorption. **a** PSs was loaded into lipid layer between OA caps of UCNPs and alkyl chain of phospholipid. (Reprinted with permission from (Thanasekaran et al. 2018). Copyright © 2018 American Chemical Society). **b** PSs was encapsulated into the hydrophobic layer between UCNPs surface and amphiphilic polymer. (Reproduced from (Wang et al. 2014) with permission from The Royal Society of Chemistry). **c** PSs was absorbed through interaction with hydrophobic pocket of BSA. (Reprinted with permission from (Chen et al. 2014b). Copyright © 2014 Elsevier)

antigens could be captured by the maleimide residue and retained in situ, enhancing the antigen uptake of antigen-presenting cells and encouraging a tumor-specific immune response. The obtained results confirmed that this concept could serve as a potential DDS for photo-immunotherapy. Not only lipids or polymers but also proteins, such as bovine serum albumin (BSA), can accommodate hydrophobic PSs. Chen and co-workers (2014) reported a protein-modified UCNP for synergistic use with PDT and PTT. BSA covalently bound to the hydrophilic PAA on the surface of UCNPs to form an amide bond in the assistant of 1-ethyl-3-(3-dimethylaminopropyl)carbodimide (EDC). RB and IR825 was encapsulated into this nanoparticle without any other coupling agent, indicating that RB and IR825 simply bind to the UCNP@BSA via a hydrophobic/hydrophobic interaction (Chen et al. 2014b). In addition, a combination of two or more PSs whose excitation peaks match the UCL spectra of UCNPs at different ranges has been considered as a strategy to improve PDT efficacy. In 2012, Idris designed mesoporous silica-coated $NaYF_4$:Yb,Er UCNPs as a transporter for two PSs: 650 nm-excited ZnPc and 540-nm-sensitized MC 540. An in vitro cytotoxicity assay indicated lower cell viability induced by the co-loaded PSs than any single PS sample (Idris et al. 2012).

However, the physical adsorption strategy has some disadvantages. Generally, hydrophobic interaction is a weak force, implying the instability and undesired leakage of encapsulated PSs. In 2012, Liu et al. presented a covalently assembled nanoplatform for imaging and PDT. The authors prepared hydrophilic UCNPs by the ligand exchange method using 2-aminoethyl dihydrogen phosphate (AEP) to take the place of oleylamine ligands and amino groups were exposed to the outermost layer. The carboxylic group of RB can then react with the primary amino functional group on the surface of UCNPs through EDC crosslinking. Moreover, folic acid (FA) was conjugated on the surface of this UCNP via bifunctional NH_2-PEG-COOH using a similar strategy to obtain a higher targeting efficacy in tumors. In comparison to most earlier studies using much higher power intensity, the covalently bonded UCNPs@PS performed a notably higher efficacy in killing cancer cells (Liu et al. 2012a). In 2015, Ai et al. also reported a UCNP-based nanoplatform using the same encapsulation tactic with a slight modification (Fig. 8). Nd^{3+} was added to the core UCNPs as a sensitizer, endowing the obtained UCNPs with an excitation wavelength at 808 nm instead of the conventional 980 nm laser source. Hence, PDT could be achieved at the center of large tumors and lead to better anticancer efficacy. The in vitro experiments showed that when KB cells were treated with FA-PEG-Ce6-UCNPs, only 43.2% remained alive after 2 min under 808-nm irradiation. This number continuously decreased to 8.3% and 1.6% when the duration of treatment increased to 5 min and 10 min, respectively (Ai et al. 2015).

Along with organic PSs, inorganic PSs have also been developed in recent years. Unfortunately, semiconductor-based material such as TiO_2 and ZnO are excited by UV light, which is strongly absorbed by normal tissues and induces phototoxicity, limiting the application

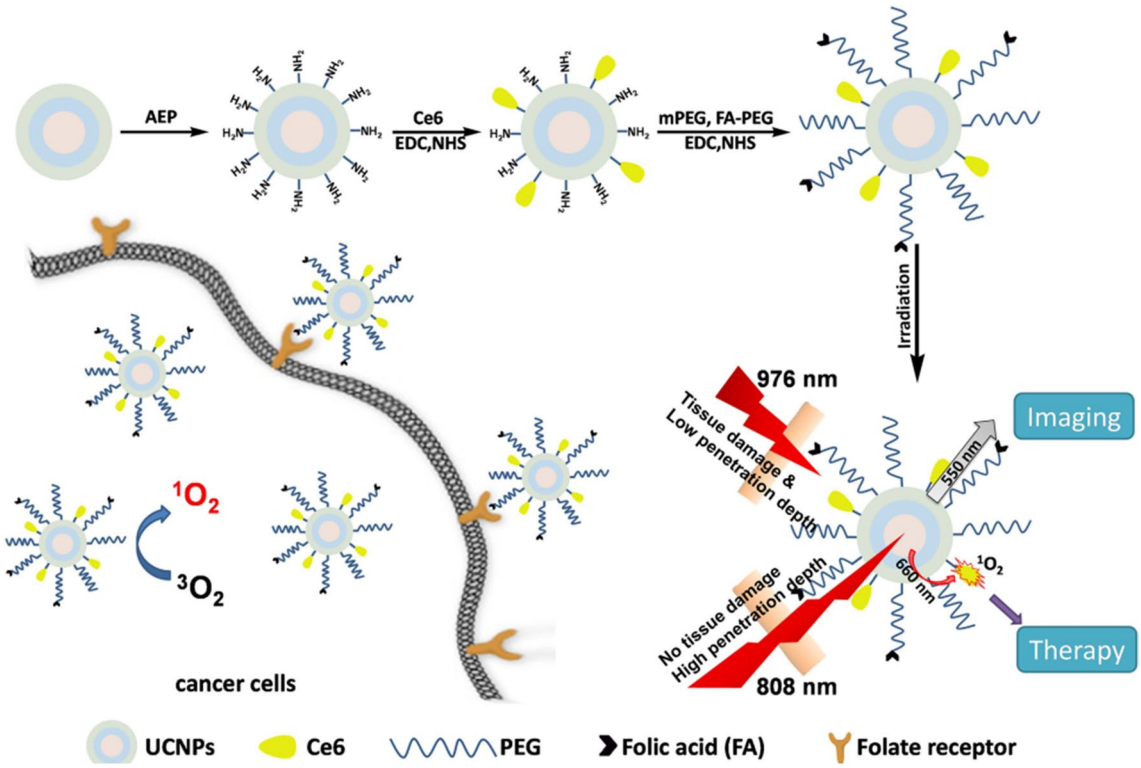

Fig. 8 Schematic illustration showing preparation of FA-PEG-Ce6-UCNPs for simultaneous PDT and bioimaging (Ai et al. 2015)

of these PSs in phototherapy. The anti-Stock shift phenomena of UCNPs affords a great opportunity to bring these UV-sensitized PSs into PDT. In 2012, Hou synthesized $NaYF_4:Yb^{3+},Tm^{3+}@NaGdF_4:Yb^{3+}$ UCNPs with the UCL that well-matched the excitation wavelength of TiO_2 shells. The UCNP@TiO_2 nanoparticles taken up by MCF-7 cancer cells generated ROS upon NIR excitation and then induced cancer cell apoptosis (Hou et al. 2015). More recently, Zhou developed a versatile nanoplatform TiO_2:Yb,Ho,F-β-CD@DTX/HA. In this concept, Yb, Ho, and F were directly doped into TiO_2 nanoparticles, which not only enhanced the PDT efficacy of TiO_2 under NIR irradiation but also overcame the poor energy transfer efficiency of the conventional UCNP@TiO_2 core/shell structure. Moreover, the synergistic effect of chemotherapy (DTX) and PDT (TiO_2) remarkably inhibited the proliferation of the MCF-7 cancer cell line as well as effectively ablated tumors at 10 days (Zhou et al. 2017).

Despite the rapid development, PDT has struggled with the resistance caused by the hypoxic tumor microenvironment, especially when it comes to solid tumors. Tumor hypoxia can take place due to either the existence of hypoxic tumor cells or the depletion of an oxygen supply that arises during PDT (Lucky et al. 2015). In 2018, Yao and co-workers introduced mesoporous cerium oxide hollow biophotocatalysts to overcome hypoxia-induced PDT

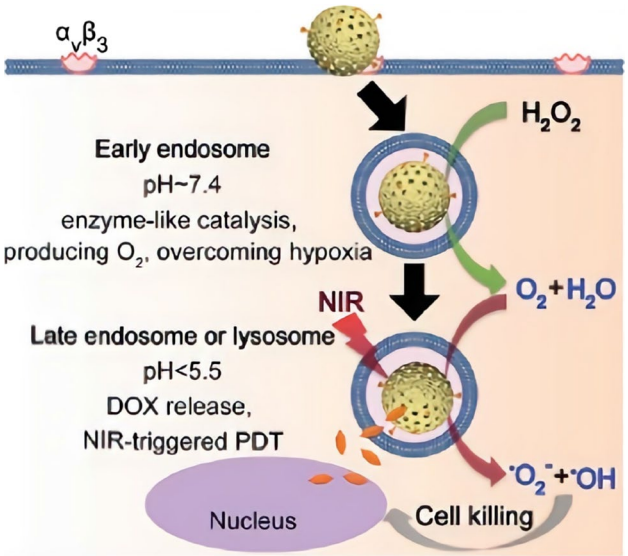

Fig. 9 Schematic illustration of the combination between chemotherapy and PDT of Ce-UCNPs overcoming hypoxia. (Reprinted with permission from (Yao et al. 2018). Copyright © 2018 WILEY-VCH Verlag GmbH & Co. KGaA, Weinheim)

resistance (Fig. 9). At first, virus-like silica nanoparticles were synthesized, followed by coating the surface of the as-synthesized nanoparticles with a Yb^{3+}, Tm^{3+}, and cerium hydroxide shell via a precipitation process. Mesoporous nanostructures were obtained after calcination and silica etching steps. In a weak acidic environment, cerium oxide can act as a catalyst for the decomposition of endogenous H_2O_2 in tumor cells and afford O_2 to enhance PDT efficacy. Furthermore, upon 980-nm NIR irradiation, Ce-UCNP emitted UV radiation to cerium oxide. Then, the photoreaction triggered the generation of ROS inducing the apoptosis of cancer cells (Yao et al. 2018).

Therapeutic applications of UCNPs with anticancer agents

Chemotherapy refers to the use of chemical compounds to efficiently kill cancer cells. After being internalized, these drugs can cause the abnormal function of cells, induce apoptosis, and damage DNA, resulting in the inhibition of proliferation and cell death. To date, chemotherapy has played a very important clinical role in cancer treatment, but there have been some drawbacks that make a complete response a tough challenge. For decades, a number of attempts have been made to improve chemotherapy efficacy, achieve target delivery, avoid adverse drug effects, minimize systemic toxicity, and overcome chemoresistance. Thanks to unique optical properties and various surface modification strategies, UCNP-based nanoplatforms have been considered as potential DDSs for chemotherapy.

NIR-triggered drug release

In 2015, Dcona and Matthew reported a system in which DOX was directly attached to the surface of UCNPs through a photocleavable linkage. First, they prepared $LiYF_4$:Tm^{3+}/Yb^{3+}-UCNPs, which had two strong emission bands at 353 nm and 368 nm under 980-nm irradiation. A photocaged DOX-dicarboxylate ligand, including nitroveratryl and glutamate residues, was synthesized. While bis-carboxylate formed a stable coordinative complex with trivalent Ln ions on the surface of UCNPs, nitroveratryl residues could be excited by the UV emission from UCNPs to cleave the

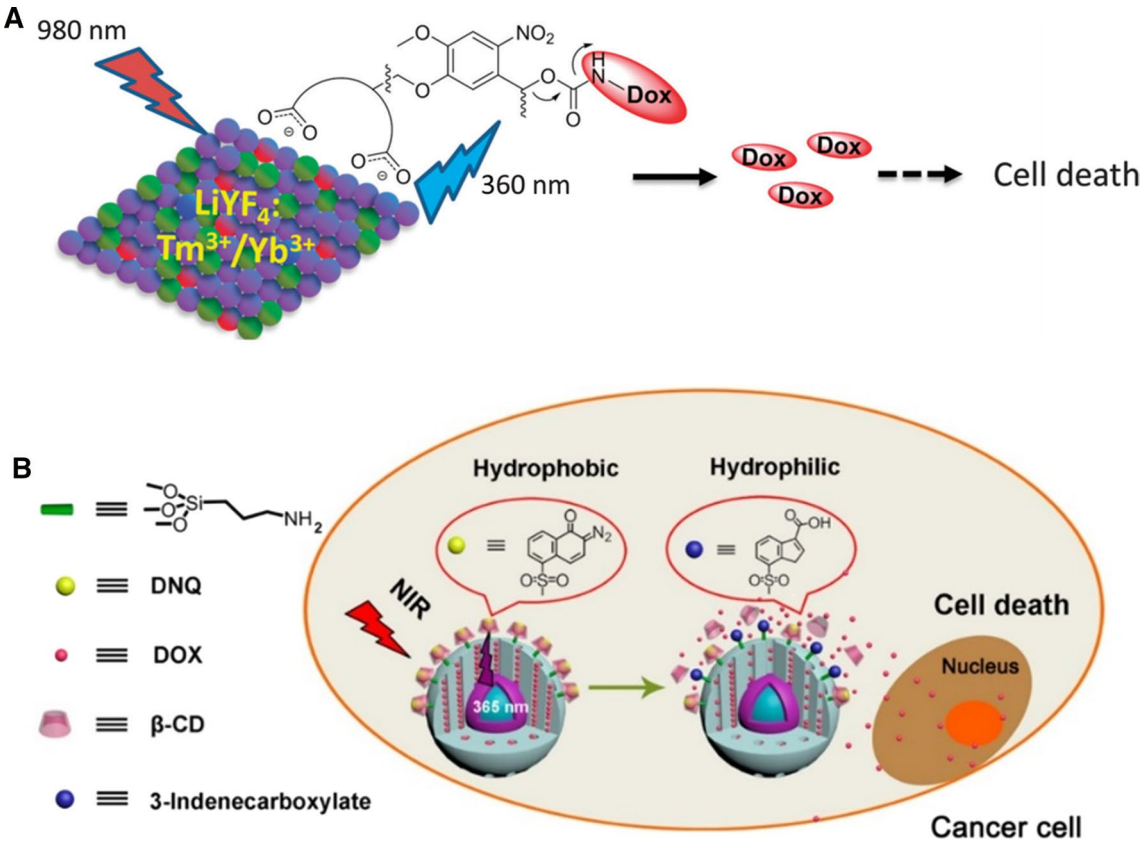

Fig. 10 Scheme for the NIR-trigger drug release. **a** Controlled release of DOX through photolabile linkers. (Reproduced from (Michael Dcona and Matthew 2015) with permission from The Royal Society of Chemistry). **b** Controlled release of DOX form drug reservoir through nanovalves. (Reprinted with permission from and (Han et al. 2018). Copyright © 2018 American Chemical Society)

pre-existing covalent bond with DOX and release free drug (Fig. 10a) (Michael Dcona and Matthew 2015).

Wang et al. suggested another NIR-triggered drug release strategy. Instead of covalent conjugate, DOX was loaded into the inner cavities of UCNP@PMAA yolk-shell structured nanocapsules. Herein, poly(methacrylic acid) (PMAA) shell, a shrinkable material, was cross-linked by bis(mathacryloylamino)azobenzene (BMAAB). UV/VIS emission from the core UCNPs upon NIR excitation can isomerize BMAAB, resulting in the tuning of the permeability via switching the status of the PMAA shell between shrinkage and swelling. Moreover, the low pH environment, pH 4.5, accelerated the release of DOX from the UCNP@PMAA yolk-shell nanostructures while almost no free DOX was observed after 8 h at pH 7 under visible light treatment (Wang et al. 2018b).

Mesoporous silica coating, which has been widely applied in UCNP-based drug delivery, not only endows UCNPs with improved dispersibility and stability in aqueous solution but also creates a sufficient cavity for drug loading. NIR-triggered drug release can be accomplished by controlling the tunnel-like pores of the mesoporous coating. He and co-workers (2015) produced mesoporous silica-coated UCNPs, which encapsulated DOX and grafted blue-light-cleavable ruthenium complexes as valves to control drug release. The $NaYF_4$:TmYb@$NaYF_4$ UCNPs could convert 974 nm excitation to 470 nm light that induced a cleavage reaction of complex Ru[(2,2′-bipyridine)2(trimethylphosphine)((3-aminopropyl) triethoxysilane)] and made the way for drug release. After 5 h irradiation (974 nm, 0.35 W/cm^2), 42% DOX was released while the absorption spectroscopy showed 59% Ru complex was cleaved from UCNP@mSiO_2 (He et al. 2015). Independently, in 2018, Han and co-workers used β-cyclodextrin (β-CD) as the gatekeeper to cap 2-diazo-1,2-naphthoquinones via hydrophobic interaction. Once exposed to UV light illumination from $NaYF_4$:TmYb@$NaYF_4$ UCNPs, hydrophobic diazo-1,2-naphthoquinones was transformed into hydrophilic 3-indenecarboxylic acid. As a result, β-CD was dissociated from the surface of UCNPs@mSiO_2 because of the repulsion between hydrophobic cavities and hydrophilic guest, followed by the release of DOX from the unblocked pores (Fig. 10B) (Han et al. 2018). The same strategy was also reported by Zhang, who used 4-(2-carboxy-ethylsulfanylmethyl)-3-nitro-benzoic acid as the UV cleavable nanovalves to control the drug release of their formulation. To enhance the tumor cellular uptake, transferrin (Tf) was conjugated onto the silica surface of UCNP@mSiO_2 (Zhang et al. 2016).

In research published by Hu in 2017, 4-arm-PEG-NH_2 was cross-linked by using an azo-containing linker to form a hydrogel, which underwent thermal degradation at temperatures above 44 °C and photolysis upon 365-nm UV light. By embedding $NaYF_4$:Yb,Tm UCNPs into the mentioned structure, the release of the DOX from the hydrogel could be triggered under 808-nm illumination (Hu et al. 2017).

NIR-triggered targeting delivery

Active targeting to deliver and accumulate drug at the tumor site with high concentration for achieving efficient therapies and avoiding systemic toxicity is a promising strategy for prospective DDSs. However, certain limitations need to be overcome, for example the heterogeneity in the expression of specific receptors among diverse cancer cells or even between tumor cells and normal cells. Chien (2013) demonstrated a NIR light photocontrolled targeting nanostructure to resolve this problem (Fig. 11). Upon the irradiation of 980 nm by a diode laser, the 360-nm photon emitted from $NaYF_4$:Yb,Tm UCNPs activated the photocleavage reaction. Then, FA was revealed after dissociating from the photolabile protecting group, 2-nitrobenzylamine, expressing targeting activity. For the chemotherapeutic effect, DOX was conjugated to the surface of UCNP@SiO_2 through an enzyme cleavable disulfide bond, leading to the photo- and enzyme-responsive efficient targeting of UCNP@SiO_2 nanoplatforms. As shown by the results of in vitro experiments, the cellular uptakes of UCNPs were illustrated through the concentration of [Y^{3+}] inside HeLa cells at 40 °C for 20 min incubation. These numbers were 5 ppm, 17 ppm, and 20 ppm for caged folate-UCNPs (without irradiation), caged folate-UCNPs (irradiation 1 min), and folate UCNPs, respectively (Chien et al. 2013).

Activation of prodrug by NIR

To date, cisplatin is one of the most popular drugs to treat different types of cancer. In spite of this, there are several drawbacks, for example severe neurotoxicity, kidney toxicity, and drug resistance that have imposed high requirements on developing safer and more efficient cisplatin delivery systems. Dai and co-workers (2013) successfully fabricated a UCNP-based multifunctional nanoplatform for bioimaging and NIR-activated cisplatin (IV) prodrug delivery (Fig. 12). The core–shell structure $NaYF_4$:$Yb^{3+/}Tm^{3+}$@$NaGdF_4$:Yb^{3+} was used to transfer NIR excitation light into 365-nm irradiation, activating the platinum(IV) prodrug, *trans,trans,trans*-[$Pt(N_3)_2(NH_3)(py)(O_2CCH_2CH_2COOH)_2$] attached on the surface of UCNPs to kill HeLa cancer cells. By using UCNPs, this formulation could achieve higher tissue penetration as well as reduce phototoxicity compared to phototherapy that directly used UV as the excitation source. In addition, UC luminescence, MRI, and CT owing to the presence of UCNP are a promising DDS for theranostics (Dai et al. 2013). Another study published in 2015 was in agreement with the use of UCNPs

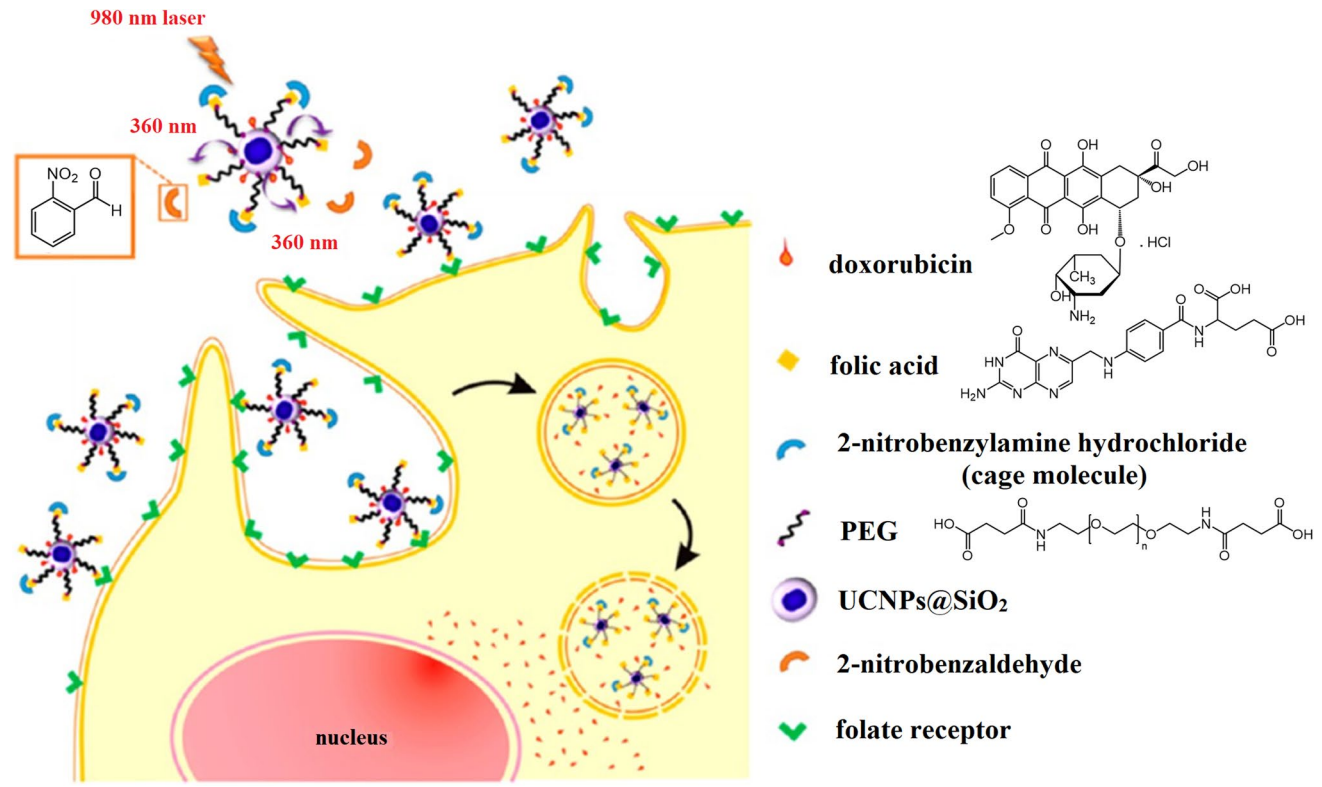

Fig. 11 Illustration of NIR-triggered targeting delivery of UCNPs@SiO_2. (Reprinted with permission from (Chien et al. 2013). Copyright © 2013 American Chemical Society)

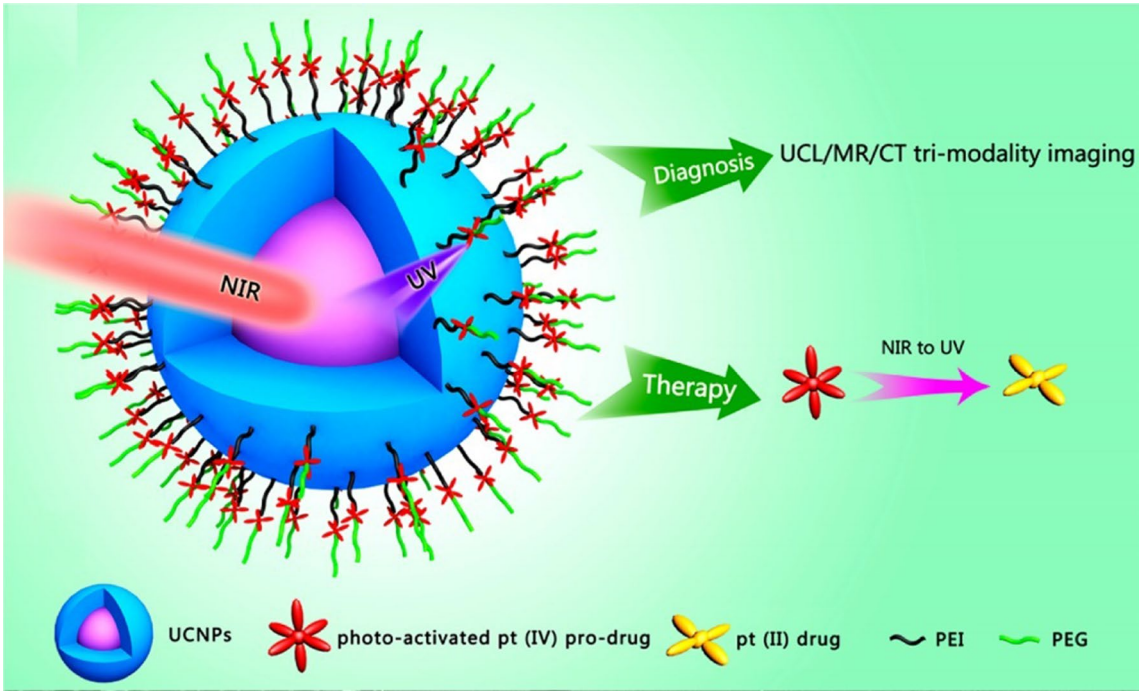

Fig. 12 Schematic illustration of the combination UCL/MR/CT tri-modality imaging and photo-activation process of UCNP-DPP-PEG nanoparticles. (Reprinted with permission from (Dai et al. 2013). Copyright © 2013 American Chemical Society)

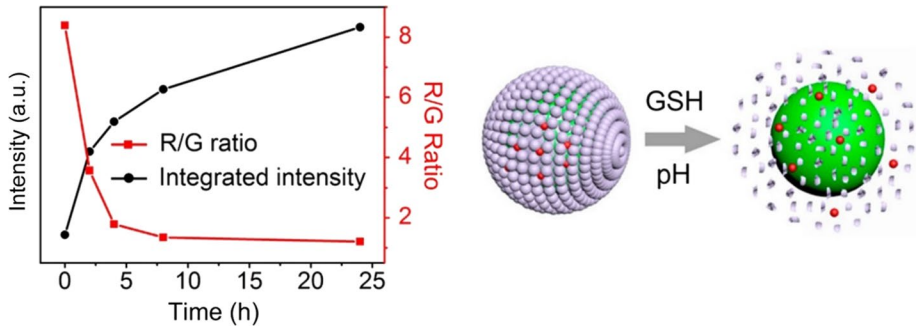

Fig. 13 Schematic illustration showing the relation between R/G ratio and the amount of DOX release from the biodegradation silica shell. (Reprinted with permission from (Xu et al. 2017c). Copyright © 2017 American Chemical Society)

to trigger the activation of Pt (IV) prodrug, *cis,cis,trans*-$[Pt(NH_3)_2(Cl)_2(O_2CCH_2CH_2CO_2H)_2]$, which was decorated on the surface of UCNPs through PEGylated phospholipid DSPE-PEG(2000)-NH_2 linkers (Ruggiero et al. 2015).

Imaging-guided drug release

Because of the fluorescence resonance energy transfer phenomenon (FRET), the green emission of UCNPs co-encapsulated with DOX tends to be hindered. Therefore, the release of DOX from UCNP-nanostructures leads to the decline of the red/green emission intensity ratio, this implies a new way to spatially and temporally detect the content of released DOX (Fig. 13) (Hu et al. 2018; Xu et al. 2017c).

In addition, the gatekeepers, β-CD, of the aforementioned UCNPs@mSiO_2 platform can conjugate to dyes, such as FITC and act as a release indicator. Before drug release, VIS emission from UCNPs was obstructed because of the luminescence resonance energy transfer phenomenon (LRET) while the detachment of β-cyclodextrin-FITC caps from the surface of UCNPs@mSiO_2 recover the UCL. Liu and co-workers also confirmed the application of LRET to quantitatively monitor the release of drug from pyrenemethyl ester-based nanovalves UCNP@mSiO_2 (Liu et al. 2019).

Combination of chemotherapy and phototherapy

Current studies have shown that the combination of chemotherapy and phototherapy can improve antitumor efficiency and overcome chemoresistance, which deprives patients of effective cancer treatment. In PDT and chemotherapy synergy, ROS from PDT can suppress the activity of the efflux translocator to render tumors affected by the chemotherapeutic effect while chemotherapy make tumors more sensitive to PDT (Khdair et al. 2009, 2010; Spring et al. 2015; Mao et al. 2018). A representative platform, TiO_2:Yb,Ho,F-β-CD@DTX/HA, for this strategy was well-described above (Zhou et al. 2017). In addition, PSs that can generate heat upon NIR irradiation have been embedded into UNCPs nanostructures to achieve PTT. In combination with chemotherapy, hyperthermia can enhance drug delivery into tumor sites as well as induce thermoablation at elevated temperature (Kim and Lee 2017; Lee et al. 2019; Phung et al. 2019). For this purpose, nanocomposite UCNPs@Au-DOXs have been developed (Fig. 14). In this procedure, gold nanocrystal, a well-known photothermal agent, was directly grown on the surface of UCNPs. Subsequently, DOX is conjugated to UCNP@Au through PEG linkers. As expected, a significant decline in cell viability was observed with the HeLa cells treated by the combination of PTT and chemotherapy (Wei et al. 2017).

Conclusion and perspectives

In this review, we have depicted the development in the surface modification, design, and bio-application of UCNPs in the last decade. Various strategies using Ln-doped UCNPs in both diagnostics and therapeutic therapy have been described in detail. The review has shown that NIR-sensitive UCNP-based nanostructures could achieve excellent spatiotemporal controlled drug release, overcome the limitations of conventional light-responsive DDSs, and act as versatile nanocarriers that have the potential of further development. Nonetheless, there are still some challenges that need to be addressed before the translation of UCNPs from academic research to clinical application. First of all, the very low UC efficiency requires a high intensity laser source, which can damage normal cells. The core–shell structures have been developed to solve this problem but inevitably increases the size of the UCNPs: the bigger size, the higher the UC efficiency. This leads to another problem because the nanoparticles need to be small in size to accumulate in targeted tumors efficiently and to be delivered into the nucleus of cells. In fact, the successful preparation of sub-10 nm UCNPs with high quantum yield has not been achieved. Therefore, the

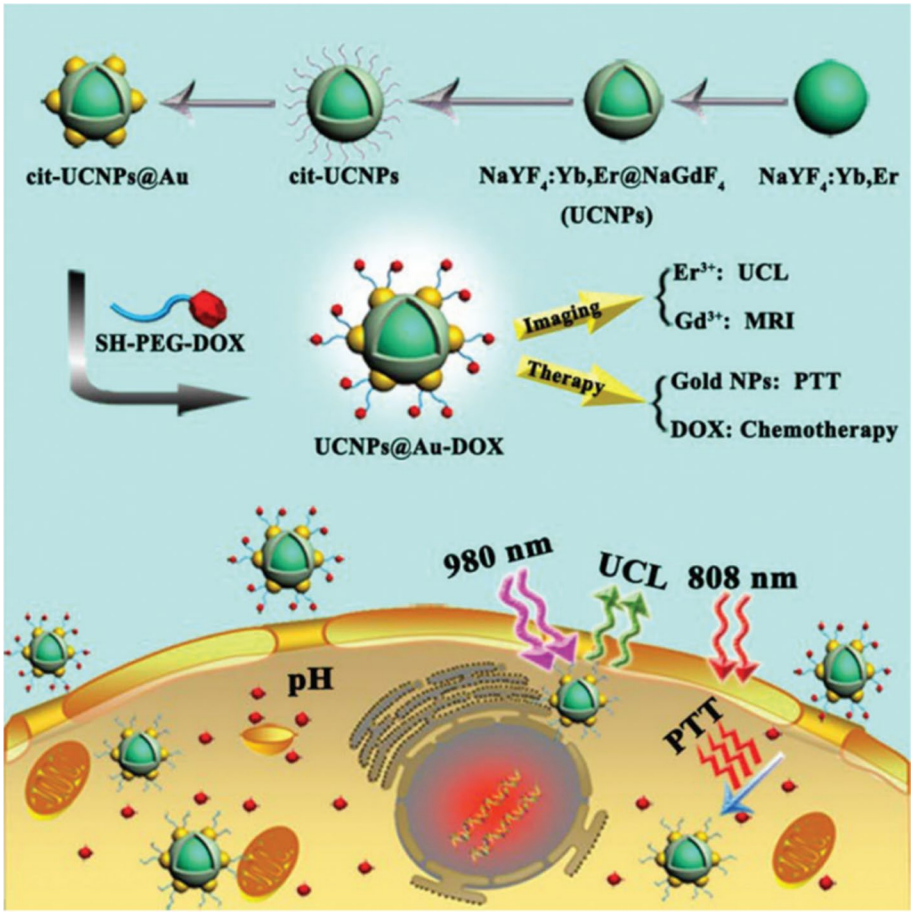

Fig. 14 Illustration of versatile UCNPs@Au-DOX nanocomposites. (Reproduced from (Wei et al. 2017) with permission from The Royal Society of Chemistry)

development of new host matrices, new structure designs, or new synthesis methods to yield UCNPs with high UC efficiency is always in high demand. Secondly, the surface modification process also affects the UC efficiency via the surface quenching phenomenon resulting from the interaction between the coating molecule and rare-earth ion on the surface of UC nanocrystals. In addition, the functional moieties attached on the surface of UCNPs play a significant role in the target delivery and circulating time of UCNPs in the human body. New surface modification strategies should be studied to maintain UC efficiency in the physiological environment as well as improve the pharmacokinetic properties of UCNP-based nanoplatforms. Thirdly, to the best of our knowledge, although most in vitro and in vivo toxicity experiments have shown that no adverse effects were observed in normal tissues and organs, the long-term toxicity of UCNPs has not been evaluated. In conclusion, this promising field is rapidly developing and there are a number of opportunities for innovatory studies.

Acknowledgements This work was supported by the National Research Foundation of Korea (NRF) Grant funded by the Korea government (MSIT) (No. NRF-2019R1A5A2027340), and a Grant (16173MFDS542) from the Ministry of Food and Drug Safety in 2019.

Compliance with ethical standards

Conflict of interest The authors declared no conflict of interest.

References

Ai F, Ju Q, Zhang X, Chen X, Wang F, Zhu G (2015) A core-shell-shell nanoplatform upconverting near-infrared light at 808 nm for luminescence imaging and photodynamic therapy of cancer. Sci Rep 5:10785. https://doi.org/10.1038/srep10785

Auzel F (2004) Upconversion and anti-Stokes processes with f and d ions in solids. Chem Rev 104:139–174. https://doi.org/10.1021/cr020357g

Bloembergen N (1959) Solid state infrared quantum counters. Phys Rev Lett 2:84–85. https://doi.org/10.1103/PhysRevLett.2.84

Bogdan N, Vetrone F, Roy R, Capobianco JA (2010) Carbohydrate-coated lanthanide-doped upconverting nanoparticles for lectin recognition. J Mater Chem 20:7543–7550. https://doi.org/10.1039/C0JM01617A

Boyer J-C, Vetrone F, Cuccia LA, Capobianco JA (2006) Synthesis of colloidal upconverting $NaYF_4$ nanocrystals doped with Er^{3+}, Yb^{3+} and Tm^{3+}, Yb^{3+} via thermal decomposition of lanthanide trifluoroacetate precursors. J Am Chem Soc 128:7444–7445. https://doi.org/10.1021/ja061848b

Cao T, Yang Y, Gao Y, Zhou J, Li Z, Li F (2011) High-quality water-soluble and surface-functionalized upconversion nanocrystals as luminescent probes for bioimaging.

Biomaterials 32:2959–2968. https://doi.org/10.1016/j.biomaterials.2010.12.050

Cen Y, Tang J, Kong X-J, Wu S, Yuan J, Yu R-Q, Chu X (2015) A cobalt oxyhydroxide-modified upconversion nanosystem for sensitive fluorescence sensing of ascorbic acid in human plasma. Nanoscale 7:13951–13957. https://doi.org/10.1039/c5nr03588k

Cheisson T, Schelter EJ (2019) Rare earth elements: Mendeleev's bane, modern marvels. Science 363:489. https://doi.org/10.1126/science.aau7628

Chen Z, Chen H, Hu H, Yu M, Li F, Zhang Q, Zhou Z, Yi T, Huang C (2008) Versatile synthesis strategy for carboxylic acid− functionalized upconverting nanophosphors as biological labels. J Am Chem Soc 130:3023–3029. https://doi.org/10.1021/ja076151k

Chen G, Qiu H, Prasad PN, Chen X (2014a) Upconversion nanoparticles: design, nanochemistry, and applications in theranostics. Chem Rev 114:5161–5214. https://doi.org/10.1021/cr400425h

Chen Q, Wang C, Cheng L, He W, Cheng Z, Liu Z (2014b) Protein modified upconversion nanoparticles for imaging-guided combined photothermal and photodynamic therapy. Biomaterials 35:2915–2923. https://doi.org/10.1016/j.biomaterials.2013.12.046

Chien Y-H, Chou Y-L, Wang S-W, Hung S-T, Liau M-C, Chao Y-J, Su C-H, Yeh C-S (2013) Near-infrared light photocontrolled targeting, bioimaging, and chemotherapy with caged upconversion nanoparticles *in vitro* and *in vivo*. ACS Nano 7:8516–8528. https://doi.org/10.1021/nn402399m

Dai Y, Xiao H, Liu J, Yuan Q, Ma PA, Yang D, Li C, Cheng Z, Hou Z, Yang P (2013) In vivo multimodality imaging and cancer therapy by near-infrared light-triggered trans-platinum pro-drug-conjugated upconverison nanoparticles. J Am Chem Soc 135:18920–18929. https://doi.org/10.1021/ja410028q

Drobizhev M, Makarov NS, Tillo SE, Hughes TE, Rebane A (2011) Two-photon absorption properties of fluorescent proteins. Nat Methods 8:393–399. https://doi.org/10.1038/nmeth.1596

Du H, Yu J, Guo D, Yang W, Wang J, Zhang B (2016) Improving the MR imaging sensitivity of upconversion nanoparticles by an internal and external incorporation of the Gd^{3+} strategy for *in vivo* tumor-targeted imaging. Langmuir 32:1155–1165. https://doi.org/10.1021/acs.langmuir.5b04186

Duan C, Liang L, Li L, Zhang R, Xu ZP (2018) Recent progress in upconversion luminescence nanomaterials for biomedical applications. J Mater Chem B 6:192–209. https://doi.org/10.1039/C7TB02527K

Fu L, Morsch M, Shi B, Wang G, Lee A, Radford R, Lu Y, Jin D, Chung R (2017) A versatile upconversion surface evaluation platform for bio–nano surface selection for the nervous system. Nanoscale 9:13683–13692. https://doi.org/10.1039/c7nr03557h

Gai S, Li C, Yang P, Lin J (2013) Recent progress in rare earth micro/nanocrystals: soft chemical synthesis, luminescent properties, and biomedical applications. Chem Rev 114:2343–2389. https://doi.org/10.1021/cr4001594

Guller AE, Generalova AN, Petersen EV, Nechaev AV, Trusova IA, Landyshev NN, Nadort A, Grebenik EA, Deyev SM, Shekhter AB (2015) Cytotoxicity and non-specific cellular uptake of bare and surface-modified upconversion nanoparticles in human skin cells. Nano Res 8:1546–1562. https://doi.org/10.1007/s12274-014-0641-6

Guo X, You J (2017) Near infrared light-controlled therapeutic molecules release of nanocarriers in cancer therapy. J Pharm Investig 47:297–316. https://doi.org/10.1007/s40005-017-0321-0

Han R-L, Shi J-H, Liu Z-J, Hou Y-F, Wang Y (2018) Near-infrared light-triggered hydrophobic-to-hydrophilic switch nanovalve for on-demand cancer therapy. ACS Biomater Sci Eng 4:3478–3486. https://doi.org/10.1021/acsbiomaterials.8b00437

He S, Krippes K, Ritz S, Chen Z, Best A, Butt H-J, Mailänder V, Wu S (2015) Ultralow-intensity near-infrared light induces drug delivery by upconverting nanoparticles. Chem Commun 51:431–434. https://doi.org/10.1039/C4CC07489K

Hou Z, Zhang Y, Deng K, Chen Y, Li X, Deng X, Cheng Z, Lian H, Li C, Lin J (2015) UV-emitting upconversion-based TiO_2 photosensitizing nanoplatform: near-infrared light mediated *in vivo* photodynamic therapy via mitochondria-involved apoptosis pathway. ACS Nano 9:2584–2599. https://doi.org/10.1021/nn506107c

Hu J, Chen Y, Li Y, Zhou Z, Cheng Y (2017) A thermo-degradable hydrogel with light-tunable degradation and drug release. Biomaterials 112:133–140. https://doi.org/10.1016/j.biomaterials.2016.10.015

Hu J, Zhan S, Wu X, Hu S, Wu S, Liu Y (2018) Core/shell upconversion nanoparticles with intense fluorescence for detecting doxorubicin *in vivo*. RSC Adv 8:21505–21512. https://doi.org/10.1039/C8RA02928H

Huang S, Cheng Z, Chen Y, Liu B, Deng X, Ma PA, Lin J (2015) Multifunctional polyelectrolyte multilayers coated onto Gd_2O_3:Yb^{3+}, E^{r3}+@MSNs can be used as drug carriers and imaging agents. RSC Adv 5:41985–41993. https://doi.org/10.1039/C5RA01750E

Hwang HS, Shin H, Han J, Na K (2018) Combination of photodynamic therapy (PDT) and anti-tumor immunity in cancer therapy. J Pharm Investig 48:143–151. https://doi.org/10.1007/s40005-017-0377-x

Idris NM, Gnanasammandhan MK, Zhang J, Ho PC, Mahendran R, Zhang Y (2012) In vivo photodynamic therapy using upconversion nanoparticles as remote-controlled nanotransducers. Nat Med 18:1580. https://doi.org/10.1038/nm.2933

Jeon G, Ko YT (2019) Enhanced photodyamic therapy via photosensitizer-loaded nanoparticles for cancer treatment. J Pharm Investig 49:1–8. https://doi.org/10.1007/s40005-017-0363-3

Johnson NJJ, Van Veggel FCJM (2013) Sodium lanthanide fluoride core-shell nanocrystals: A general perspective on epitaxial shell growth. Nano Res 6:547–561. https://doi.org/10.1007/s12274-013-0333-7

Kang H, Zhang K, Wong DSH, Han F, Li B, Bian L (2018) Near-infrared light-controlled regulation of intracellular calcium to modulate macrophage polarization. Biomaterials 178:681–696. https://doi.org/10.1016/j.biomaterials.2018.03.007

Khdair A, Handa H, Mao G, Panyam J (2009) Nanoparticle-mediated combination chemotherapy and photodynamic therapy overcomes tumor drug resistance *in vitro*. Eur J Pharm Biopharm 71:214–222. https://doi.org/10.1016/j.ejpb.2008.08.017

Khdair A, Chen D, Patil Y, Ma L, Dou QP, Shekhar MP, Panyam J (2010) Nanoparticle-mediated combination chemotherapy and photodynamic therapy overcomes tumor drug resistance. J Control Release 141:137–144. https://doi.org/10.1016/j.jconrel.2009.09.004

Kim HS, Lee DY (2017) Photothermal therapy with gold nanoparticles as an anticancer medication. J Pharm Investig 47:19–26. https://doi.org/10.1007/s40005-016-0292-6

Lai J, Shah BP, Zhang Y, Yang L, Lee K-B (2015) Real-time monitoring of ATP-responsive drug release using mesoporous-silica-coated multicolor upconversion nanoparticles. ACS Nano 9:5234–5245. https://doi.org/10.1021/acsnano.5b00641

Le Q-V, Choi J, Oh Y-K (2018) Nano delivery systems and cancer immunotherapy. J Pharm Investig 48:527–539. https://doi.org/10.1007/s40005-018-0399-z

Lee C, Lim K, Kim SS, Lee ES, Oh KT, Choi H-G, Youn YS (2019) Chlorella-gold nanorods hydrogels generating photosynthesis-derived oxygen and mild heat for the treatment of hypoxic breast cancer. J Control Release 294:77–90. https://doi.org/10.1016/j.jconrel.2018.12.011

Li C, Lin J (2010) Rare earth fluoride nano-/microcrystals: synthesis, surface modification and application. J Mater Chem 20:6831–6847. https://doi.org/10.1039/C0JM00031K

Li Z, Zhang Y (2008) An efficient and user-friendly method for the synthesis of hexagonal-phase $NaYF_4$:Yb, Er/Tm nanocrystals with controllable shape and upconversion fluorescence. Nanotechnology 19:345606. https://doi.org/10.1088/0957-4484/19/34/345606

Li Z, Zhang Y, Jiang S (2008) Multicolor core/shell-structured upconversion fluorescent nanoparticles. Adv Mater 20:4765–4769. https://doi.org/10.1002/adma.200801056

Li X, Zhang F, Zhao D (2015) Lab on upconversion nanoparticles: optical properties and applications engineering via designed nanostructure. Chem Soc Rev 44:1346–1378. https://doi.org/10.1039/C4CS00163J

Li Q, Li X, Zhang L, Zuo J, Zhang Y, Liu X, Tu L, Xue B, Chang Y, Kong X (2018) An 800 nm driven $NaErF_4$@$NaLuF_4$ upconversion platform for multimodality imaging and photodynamic therapy. Nanoscale 10:12356–12363. https://doi.org/10.1039/C8NR00446C

Liang S, Zhang X, Wu Z, Liu Y, Zhang H, Sun H, Sun H, Yang B (2012) Decoration of up-converting $NaYF_4$: Yb, Er (Tm) nanoparticles with surfactant bilayer. A versatile strategy to perform oil-to-water phase transfer and subsequently surface silication. CrystEngComm 14:3484–3489. https://doi.org/10.1039/C2CE06578A

Liang L, Lu Y, Zhang R, Care A, Ortega TA, Deyev SM, Qian Y, Zvyagin AV (2017) Deep-penetrating photodynamic therapy with KillerRed mediated by upconversion nanoparticles. Acta Biomater 51:461–470. https://doi.org/10.1016/j.actbio.2017.01.004

Lin Z, Vučković J (2010) Enhanced two-photon processes in single quantum dots inside photonic crystal nanocavities. Phys Rev B 81:035301. https://doi.org/10.1103/PhysRevB.81.035301

Lin M, Gao Y, Diefenbach TJ, Shen JK, Hornicek FJ, Park YI, Xu F, Lu TJ, Amiji M, Duan Z (2017) Facial layer-by-layer engineering of upconversion nanoparticles for gene delivery: near-infrared-initiated fluorescence resonance energy transfer tracking and overcoming drug resistance in ovarian cancer. ACS Appl Bio Mater 9:7941–7949. https://doi.org/10.1021/acsami.6b15321

Lingeshwar Reddy K, Balaji R, Kumar A, Krishnan V (2018) Lanthanide doped near infrared active upconversion nanophosphors: Fundamental concepts, synthesis strategies, and technological applications. Small 14:1801304. https://doi.org/10.1002/smll.201801304

Liu X, Zhao J, Sun Y, Song K, Yu Y, Du C, Kong X, Zhang H (2009) Ionothermal synthesis of hexagonal-phase $NaYF_4$:Yb^{3+},Er^{3+}/Tm^{3+} upconversion nanophosphors. Chem Commun. https://doi.org/10.1039/B915517A.

Liu Q, Chen M, Sun Y, Chen G, Yang T, Gao Y, Zhang X, Li F (2011a) Multifunctional rare-earth self-assembled nanosystem for tri-modal upconversion luminescence/fluorescence/positron emission tomography imaging. Biomaterials 32:8243–8253. https://doi.org/10.1016/j.biomaterials.2011.07.053

Liu Q, Sun Y, Yang T, Feng W, Li C, Li F (2011b) Sub-10 nm hexagonal lanthanide-doped $NaLuF_4$ upconversion nanocrystals for sensitive bioimaging *in vivo*. J Am Chem Soc 133:17122–17125. https://doi.org/10.1021/ja207078s

Liu K, Liu X, Zeng Q, Zhang Y, Tu L, Liu T, Kong X, Wang Y, Cao F, Lambrechts SA (2012a) Covalently assembled NIR nanoplatform for simultaneous fluorescence imaging and photodynamic therapy of cancer cells. ACS Nano 6:4054–4062. https://doi.org/10.1021/nn300436b

Liu Y, Ai K, Liu J, Yuan Q, He Y, Lu L (2012b) A high-performance ytterbium-based nanoparticulate contrast agent for *in vivo* X-ray computed tomography imaging. Angew Chem Int Ed Engl 51:1437–1442. https://doi.org/10.1002/anie.201106686

Liu Y, Ai K, Liu J, Yuan Q, He Y, Lu L (2012c) Hybrid $BaYbF_5$ nanoparticles: novel binary contrast agent for high-resolution *in vivo* X-ray computed tomography angiography. Adv Healthc Mater 1:461–466. https://doi.org/10.1002/adhm.201200028

Liu Q, Feng W, Yang T, Yi T, Li F (2013) Upconversion luminescence imaging of cells and small animals. Nat Protoc 8:2033. https://doi.org/10.1038/nprot.2013.114

Liu C, Zhang Y, Liu M, Chen Z, Lin Y, Li W, Cao F, Liu Z, Ren J, Qu X (2017) A NIR-controlled cage mimicking system for hydrophobic drug mediated cancer therapy. Biomaterials 139:151–162. https://doi.org/10.1016/j.biomaterials.2017.06.008

Liu M, Shi Z, Wang X, Zhang Y, Mo X, Jiang R, Liu Z, Fan L, Ma C-G, Shi F (2018) Simultaneous enhancement of red upconversion luminescence and CT contrast of $NaGdF_4$: Yb, Er nanoparticles via Lu^{3+} doping. Nanoscale 10:20279–20288. https://doi.org/10.1039/C8NR06968A

Liu Z, Shi J, Wang Y, Gan Y, Wan P (2019) Facile preparation of pyrenemethyl ester-based nanovalve on mesoporous silica coated upconversion nanoparticle for NIR light-triggered drug release with potential monitoring capability. Colloids Surf A 568:436–444. https://doi.org/10.1016/j.colsurfa.2019.02.027

Lu S, Tu D, Hu P, Xu J, Li R, Wang M, Chen Z, Huang M, Chen X (2015) Multifunctional nano-bioprobes based on rattle-structured upconverting luminescent nanoparticles. Angew Chem Int Ed Engl 54:7915–7919. https://doi.org/10.1002/anie.201501468

Lucky SS, Soo KC, Zhang Y (2015) Nanoparticles in photodynamic therapy. Chem Rev 115:1990–2042. https://doi.org/10.1021/cr5004198

Lv R, Wang D, Xiao L, Chen G, Xia J, Prasad PN (2017) Stable ICG-loaded upconversion nanoparticles: silica core/shell theranostic nanoplatform for dual-modal upconversion and photoacoustic imaging together with photothermal therapy. Sci Rep 7:15753. https://doi.org/10.1038/s41598-017-16016-x

Lv R, Feng M, Xiao L, Damasco JA, Tian J, Prasad PN (2018) Multilevel nanoarchitecture exhibiting biosensing for cancer diagnostics by dual-modal switching of optical and magnetic resonance signals. ACS Appl Bio Mater 1:1505–1511. https://doi.org/10.1021/acsabm.8b00429

Mai H-X, Zhang Y-W, Si R, Yan Z-G, Sun L-D, You L-P, Yan C-H (2006) High-quality sodium rare-earth fluoride nanocrystals: controlled synthesis and optical properties. J Am Chem Soc 128:6426–6436. https://doi.org/10.1021/ja060212h

Mai H-X, Zhang Y-W, Sun L-D, Yan C-H (2007) Size-and phase-controlled synthesis of monodisperse $NaYF_4$: Yb, Er nanocrystals from a unique delayed nucleation pathway monitored with upconversion spectroscopy. J Phys Chem C 111:13730–13739. https://doi.org/10.1021/jp073919e

Maji SK, Sreejith S, Joseph J, Lin M, He T, Tong Y, Sun H, Yu SWK, Zhao Y (2014) Upconversion nanoparticles as a contrast agent for photoacoustic imaging in live mice. Adv Mater 26:5633–5638. https://doi.org/10.1002/adma.201400831

Mao C, Li F, Zhao Y, Debinski W, Ming X (2018) P-glycoprotein-targeted photodynamic therapy boosts cancer nanomedicine by priming tumor microenvironment. Theranostics 8:6274. https://doi.org/10.7150/thno.29580

Michael Dcona M, Matthew C (2015) Near infrared light mediated release of doxorubicin using upconversion nanoparticles. Chem Commun 51:8477–8479. https://doi.org/10.1039/C5CC01795E

Mura S, Nicolas J, Couvreur P (2013) Stimuli-responsive nanocarriers for drug delivery. Nat Mater 12:991. https://doi.org/10.1038/nmat3776

Naccache R, Vetrone F, Mahalingam V, Cuccia LA, Capobianco JA (2009) Controlled synthesis and water dispersibility of hexagonal phase $NaGdF_4$:Ho^{3+}/Yb^{3+} nanoparticles. Chem Mater 21:717–723. https://doi.org/10.1021/cm803151y

Pacheco EM, De Araujo CB (1988) Frequency up-conversion in a borate glass doped with Pr^{3+}. Chem Phys Lett 148:334–336. https://doi.org/10.1016/0009-2614(88)87283-X

Park O, Yu G, Jung H, Mok H (2017) Recent studies on micro-/nano-sized biomaterials for cancer immunotherapy. J Pharm Investig 47:11–18. https://doi.org/10.1007/s40005-016-0288-2

Patra A, Friend CS, Kapoor R, Prasad PN (2003) Fluorescence upconversion properties of Er^{3+}-doped TiO_2 and $BaTiO_3$ nanocrystallites. Chem Mater 15:3650–3655. https://doi.org/10.1021/cm020897u

Peng J, Sun Y, Zhao L, Wu Y, Feng W, Gao Y, Li F (2013) Polyphosphoric acid capping radioactive/upconverting $NaLuF_4$: Yb, Tm, ^{153}Sm nanoparticles for blood pool imaging *in vivo*. Biomaterials 34:9535–9544. https://doi.org/10.1016/j.biomaterials.2013.07.098

Phung DC, Nguyen HT, Phuong Tran TT, Jin SG, Yong CS, Truong DH, Tran TH, Kim JO (2019) Combined hyperthermia and chemotherapy as a synergistic anticancer treatment. J Pharm Investig 49:519–526. https://doi.org/10.1007/s40005-019-00431-5

Rieffel J, Chen F, Kim J, Chen G, Shao W, Shao S, Chitgupi U, Hernandez R, Graves SA, Nickles RJ (2015) Hexamodal imaging with porphyrin-phospholipid-coated upconversion nanoparticles. Adv Mater 27:1785–1790. https://doi.org/10.1002/adma.201404739

Ruggiero E, Hernández-Gil J, Mareque-Rivas JC, Salassa L (2015) Near infrared activation of an anticancer Pt^{IV} complex by Tm-doped upconversion nanoparticles. Chem Commun 51:2091–2094. https://doi.org/10.1039/C4CC07960D

Rumi M, Perry JW (2010) Two-photon absorption: an overview of measurements and principles. Adv Opt Photonics 2:451–518. https://doi.org/10.1364/AOP.2.000451

Seo HJ, Nam SH, Im H-J, Park J-Y, Lee JY, Yoo B, Lee Y-S, Jeong JM, Hyeon T, Kim JW (2015) Rapid hepatobiliary excretion of micelle-encapsulated/radiolabeled upconverting nanoparticles as an integrated form. Sci Rep 5:15685. https://doi.org/10.1038/srep15685

Shen J, Chen G, Vu AM, Fan W, Bilsel OS, Chang CC, Han G (2013) Engineering the upconversion nanoparticle excitation wavelength: cascade sensitization of tri-doped upconversion colloidal nanoparticles at 800 nm. Adv Opt Mater 1:644–650. https://doi.org/10.1002/adom.201300160

Shi Y, Shi B, Dass AVE, Lu Y, Sayyadi N, Kautto L, Willows RD, Chung R, Piper J, Nevalainen H (2016) Stable upconversion nanohybrid particles for specific prostate cancer cell immunodetection. Sci Rep 6:37533. https://doi.org/10.1038/srep37533

Spring BQ, Rizvi I, Xu N, Hasan T (2015) The role of photodynamic therapy in overcoming cancer drug resistance. Photochem Photobiol Sci 14:1476–1491. https://doi.org/10.1039/C4PP00495G

Sun Y, Zhang W, Wang B, Xu X, Chou J, Shimoni O, Ung AT, Jin D (2018) A supramolecular self-assembly strategy for upconversion nanoparticle bioconjugation. Chem Commun 54:3851–3854. https://doi.org/10.1039/C8CC00708J

Tanabe S, Ohyagi T, Soga N, Hanada T (1992) Compositional dependence of Judd-Ofelt parameters of Er^{3+} ions in alkali-metal borate glasses. Phys Rev B 46:3305–3310. https://doi.org/10.1103/PhysRevB.46.3305

Thanasekaran P, Chu C-H, Wang S-B, Chen K-Y, Gao H-D, Lee MM, Sun S-S, Li J-P, Chen J-Y, Chen J-K (2018) Lipid-wrapped upconversion nanoconstruct/photosensitizer complex for near-infrared light-mediated photodynamic therapy. ACS Appl Mater Interfaces 11:84–95. https://doi.org/10.1021/acsami.8b07760

Tian G, Zheng X, Zhang X, Yin W, Yu J, Wang D, Zhang Z, Yang X, Gu Z, Zhao Y (2015) TPGS-stabilized $NaYbF_4$: Er upconversion nanoparticles for dual-modal fluorescent/CT imaging and anticancer drug delivery to overcome multi-drug resistance. Biomaterials 40:107–116. https://doi.org/10.1016/j.biomaterials.2014.11.022

Tsoi KM, Dai Q, Alman BA, Chan WCW (2013) Are quantum dots toxic? Exploring the discrepancy between cell culture and animal studies. Acc Chem Res 46:662–671. https://doi.org/10.1021/ar300040z

Wang L, Li Y (2007) Controlled synthesis and luminescence of lanthanide doped $NaYF_4$ nanocrystals. Chem Mater 19:727–734. https://doi.org/10.1021/cm061887m

Wang L, Yan R, Huo Z, Wang L, Zeng J, Bao J, Wang X, Peng Q, Li Y (2005a) Fluorescence resonant energy transfer biosensor based on upconversion-luminescent nanoparticles. Angew Chem Int Ed Engl 44:6054–6057. https://doi.org/10.1002/anie.200501907

Wang X, Zhuang J, Peng Q, Li Y (2005b) A general strategy for nanocrystal synthesis. Nature 437:121–124. https://doi.org/10.1038/nature03968

Wang G, Peng Q, Li Y (2009) Upconversion luminescence of monodisperse CaF_2: Yb^{3+}/Er^{3+} nanocrystals. J Am Chem Soc 131:14200–14201. https://doi.org/10.1021/ja906732y

Wang C, Cheng L, Xu H, Liu Z (2012) Towards whole-body imaging at the single cell level using ultra-sensitive stem cell labeling with oligo-arginine modified upconversion nanoparticles. Biomaterials 33:4872–4881. https://doi.org/10.1016/j.biomaterials.2012.03.047

Wang X, Liu K, Yang G, Cheng L, He L, Liu Y, Li Y, Guo L, Liu Z (2014) Near-infrared light triggered photodynamic therapy in combination with gene therapy using upconversion nanoparticles for effective cancer cell killing. Nanoscale 6:9198–9205. https://doi.org/10.1039/C4NR02495H

Wang D, Zhu L, Pu Y, Wang J-X, Chen J-F, Dai L (2017) Transferrin-coated magnetic upconversion nanoparticles for efficient photodynamic therapy with near-infrared irradiation and luminescence bioimaging. Nanoscale 9:11214–11221. https://doi.org/10.1039/C7NR03019C

Wang M, Hou Z, Al Kheraif AA, Xing B, Lin J (2018a) Mini review of TiO_2-based multifunctional nanocomposites for near-infrared light–responsive phototherapy. Adv Healthc Mater 7:1800351. https://doi.org/10.1002/adhm.201800351

Wang X, Liu X, Wang L, Tang C-Y, Law W-C, Zhang G, Liao Y, Liu C, Liu Z (2018b) Synthesis of yolk–shell polymeric nanocapsules encapsulated with monodispersed upconversion nanoparticle for dual-responsive controlled drug release. Macromolecules 51:10074–10082. https://doi.org/10.1021/acs.macromol.8b01770

Wang M, Song J, Zhou F, Hoover AR, Murray C, Zhou B, Wang L, Qu J, Chen WR (2019) NIR-triggered phototherapy and immunotherapy via an antigen-capturing nanoplatform for metastatic cancer treatment. Adv Sci (Weinh) 6:1802157. https://doi.org/10.1002/advs.201802157

Wei R, Xi W, Wang H, Liu J, Mayr T, Shi L, Sun L (2017) In situ crystal growth of gold nanocrystals on upconversion nanoparticles for synergistic chemo-photothermal therapy. Nanoscale 9:12885–12896. https://doi.org/10.1039/C7NR02280H

Wu Z, Guo C, Liang S, Zhang H, Wang L, Sun H, Yang B (2012) A pluronic F127 coating strategy to produce stable up-conversion $NaYF_4$:Yb, Er(Tm) nanoparticles in culture media for bioimaging. J Mater Chem 22:18596–18602. https://doi.org/10.1039/C2JM33626J

Wu Y, Li D, Zhou F, Liang H, Liu Y, Hou W, Yuan Q, Zhang X, Tan W (2018) Versatile in situ synthesis of MnO_2 nanolayers on upconversion nanoparticles and their application in activatable fluorescence and MRI imaging. Chem Sci 9:5427–5434. https://doi.org/10.1039/C8SC00490K

Xiang J, Tong X, Shi F, Karsenti P-L, Zhao Y (2016) Spatial organization and optical properties of layer-by-layer assembled

upconversion and gold nanoparticles in thin films. J Mater Chem C Mater 4:9343–9349. https://doi.org/10.1039/C6TC03066A

Xiao Q, Li Y, Li F, Zhang M, Zhang Z, Lin H (2014) Rational design of a thermalresponsive-polymer-switchable FRET system for enhancing the temperature sensitivity of upconversion nanophosphors. Nanoscale 6:10179–10186. https://doi.org/10.1039/C4NR02497D

Xing H, Zhang S, Bu W, Zheng X, Wang L, Xiao Q, Ni D, Zhang J, Zhou L, Peng W (2014) Ultrasmall $NaGdF_4$ nanodots for efficient MR angiography and atherosclerotic plaque imaging. Adv Mater 26:3867–3872. https://doi.org/10.1002/adma.201305222

Xu J, Yang P, Sun M, Bi H, Liu B, Yang D, Gai S, He F, Lin J (2017a) Highly emissive dye-sensitized upconversion nanostructure for dual-photosensitizer photodynamic therapy and bioimaging. ACS Nano 11:4133–4144. https://doi.org/10.1021/acsnano.7b00944

Xu J, Gulzar A, Liu Y, Bi H, Gai S, Liu B, Yang D, He F, Yang P (2017b) Integration of IR-808 sensitized upconversion nanostructure and MoS_2 nanosheet for 808 nm NIR light triggered phototherapy and bioimaging. Small 13:1701841. https://doi.org/10.1002/smll.201701841

Xu J, He F, Cheng Z, Lv R, Dai Y, Gulzar A, Liu B, Bi H, Yang D, Gai S (2017c) Yolk-structured upconversion nanoparticles with biodegradable silica shell for FRET sensing of drug release and imaging-guided chemotherapy. Chem Mater 29:7615–7628. https://doi.org/10.1021/acs.chemmater.7b03461

Yao C, Wang W, Wang P, Zhao M, Li X, Zhang F (2018) Near-infrared upconversion mesoporous cerium oxide hollow biophotocatalyst for voncurrent pH-/H_2O_2-responsive O_2-evolving synergetic cancer therapy. Adv Mater 30:1704833. https://doi.org/10.1002/adma.201704833

Yi G-S, Chow G-M (2007) Water-soluble $NaYF_4$:Yb, Er(Tm)/NaY_F4/polymer core/shell/shell nanoparticles with significant enhancement of upconversion fluorescence. Chem Mater 19:341–343. https://doi.org/10.1021/cm062447y

Yi G, Lu H, Zhao S, Ge Y, Yang W, Chen D, Guo L-H (2004) Synthesis, characterization, and biological application of size-controlled nanocrystalline $NaYF_4$:Yb, Er infrared-to-visible up-conversion phosphors. Nano Lett 4:2191–2196. https://doi.org/10.1021/nl048680h

Youn YS, Kwag DS, Lee ES (2017) Multifunctional nano-sized fullerenes for advanced tumor therapy. J Pharm Investig 47:1–10. https://doi.org/10.1007/s40005-016-0282-8

Zhang G, Liu Y, Yuan Q, Zong C, Liu J, Lu L (2011) Dual modal *in vivo* imaging using upconversion luminescence and enhanced computed tomography properties. Nanoscale 3:4365–4371. https://doi.org/10.1039/C1NR10736D

Zhang T, Lin H, Cui L, An N, Tong R, Chen Y, Yang C, Li X, Qu F (2016) NIR-sensitive UCNP@mSiO_2 nanovehicles for on-demand drug release and photodynamic therapy. RSC Adv 6:26479–26489. https://doi.org/10.1039/C6RA03186B

Zhang D, Wei L, Zhong M, Xiao L, Li H-W, Wang J (2018) The morphology and surface charge-dependent cellular uptake efficiency of upconversion nanostructures revealed by single-particle optical microscopy. Chem Sci 9:5260–5269. https://doi.org/10.1039/C8SC01828F

Zheng Q, Jockusch S, Zhou Z, Altman RB, Warren JD, Turro NJ, Blanchard SC (2012) On the mechanisms of cyanine fluorophore photostabilization. J Phys Chem Lett 3:2200–2203. https://doi.org/10.1021/jz300670p

Zhong Y, Rostami I, Wang Z, Dai H, Hu Z (2015) Energy migration engineering of bright rare-earth upconversion nanoparticles for excitation by light-emitting diodes. Adv Mater 27:6418–6422. https://doi.org/10.1002/adma.201502272

Zhou J, Luo P, Sun C, Meng L, Ye W, Chen S, Du B (2017) A "win–win" nanoplatform: TiO_2: Yb, Ho, F for NIR light-induced synergistic therapy and imaging. Nanoscale 9:4244–4254. https://doi.org/10.1039/C6NR09717K